GEOFIZIKAI
KÖZLEMÉNYEK

GEOPHYSICAL
TRANSACTIONS

CONTENTS

ELGI

BUDAPEST

TARTALOM

СОДЕРЖАНИЕ

GENERAL THEOREM ON MEAN WAVE ATTENUATION

Gábor KORVIN*

In 1980 AKI conclusively demonstrated that the quality factor Q for shear waves in the crust and upper mantle increases with frequency over the range 1–25 Hz, in contradistinction to earlier assumptions and theories on the constancy of Q. The aim of the present paper is to show that this phenomenon can be explained within the framework of the mean field concept of random wave propagation theory. A general asymptotic formula is derived for the high-frequency behaviour of the mean field attenuation coefficient and, as an application of this general formula, it is shown that for plausible models of the random velocity fluctuation the mean field approximation provides a frequency-dependence of Q that is compatible with AKI's data.

d: wave propagation, attenuation, models, velocity fluctuation

1. Introduction and problem discussion

The constancy of Q over a broad frequency range has been widely accepted by seismologists since KNOPOFF's [1964] important review on the subject. In exploration seismology ATTEWELL–RAMANA [1966] also compiled a large number of published data proving a nearly linear frequency-dependence of the coefficient of absorption. (The definitions of the quality factor Q, absorption coefficient a and of other measures of attenuation are summarized in BRADLEY–FORT [1966]. The quality factor Q and a are connected by Eq. (34) of the present paper.) In the last decade, however, several papers have been published reporting evidence on or assumptions about a possible frequency-dependence of Q [in seismology TSAI–AKI 1969, SOLOMON 1972, NUR 1971, LEE–SOLOMON 1978, etc.; in exploration seismology BODOKY et al. 1971, CROWE–ALHILALI 1975, PETROVICS et al. 1975; in rock physics AUBERGER–RINEHART 1961, MILITZER–STOLL 1968, MILITZER–SCHÖN 1972].

A recent paper of AKI [1980] has gained considerable attention. This paper, based on an analysis of the filtered records of some 900 earthquakes occurring in the region of central Japan with focal depths to 150 km, and on some earlier findings of FEDOTOV–BOLDYREV [1969] and RAUTIAN–KHALTURIN [1978], conclusively demonstrates that Q for the shear waves in the crust and upper mantle increases with frequency over the range 1–25 Hz, at least in the areas studied. Since the publication of AKI's paper several works have been devoted to explaining these findings and to revising the existing absorption—scattering theories [AKI 1981; KIKUCHI 1981; DAINTY 1981; SATO 1982a, 1982b; WU 1982]. Following an approach of WARREN [1972], DAINTY [1981] fitted AKI's Q [ω] data between 1 and 30 Hz by

* Eötvös Loránd Geophysical Institute of Hungary, POB 35. Budapest, H-1440

$$\frac{1}{Q(\omega)} = \frac{1}{Q_i} + g_0 \frac{v}{\omega} \tag{1}$$

with Q_i being the intrinsic Q [$Q_i = 2000$], v the shear wave velocity [assumed to be 3.5 km/sec], $g_0 = 0.01$ km^{-1} for the observations in Japan and $g_0 = = 0.005$ km^{-1} for Central Asia.

The original data of AKI [1980] are reproduced in *Fig. 1*. The frequency dependence of Q^{-1} is similar to that obtained by a simple relaxation model, with the peak around 0.5 Hz. The descending flank of the curve for frequencies higher than 0.75 Hz is fitted by AKI [1980] by a $Q^{-1} = \text{const} \cdot f^{-0.6}$ law, as against DAINTY's Eq. (1).
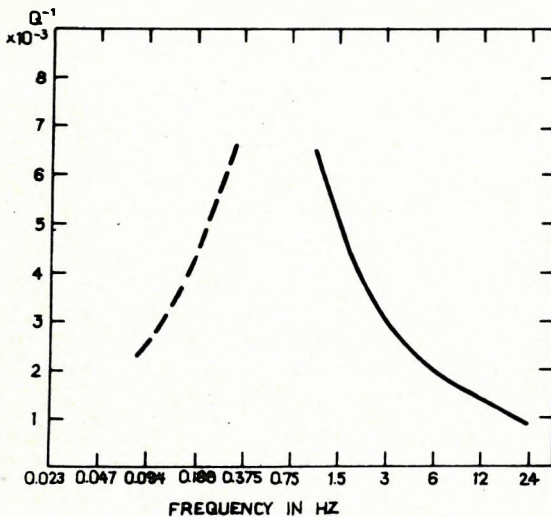
Fig. 1. Frequency dependence of Q^{-1} (after AKI 1980)

1. ábra. A Q^{-1} frekvencia-függése (AKI 1980 nyomán)

Рис. 1. Зависимость Q^{-1} от частоты (по Аки, 1980 г.)

In his 1980-paper AKI analysed a number of absorption mechanisms and has found that most of them are not compatible with his earthquake data. In view of this he ruled out the frictional energy dissipation on sliding crack surfaces, the viscous damping due to liquids in cracks, the dislocation glide, etc., and he found the thermoelastic effect or scattering due to inclusions and cracks to be the most viable models.

A possible explanation of AKI's findings is provided in a recent paper of WU [1982], who tries to explain the frequency-dependence of Q^{-1} by a simplified multiple-scattering approach. WU begins his paper with a criticism of the single scattering theories and of the mean field concept. First, he even queries the physical reality of the concept of "mean fields" in random wave propagation theory and claims that the "attenuation of the mean field is in fact only a statistical effect that measures the rate of randomization for waves passing through a random medium" and "the usual comparison between the measured attenuation of amplitude and the calculated mean field attenuations cannot produce meaningful results". WU bases this assumption on his *Fig. 3* which

suggests that the mean field formalism would result in a Q^{-1} (f) function infinitely increasing with frequency, in obvious contradiction to AKI's data. (See also SATO 1982a, 1982b.)

For low frequencies the agreement of the mean field formulation with conventional scattering theory has already been shown, in a particular case, in KORVIN [1980]. In the present paper we shall derive a general asymptotic formula for the high-frequency behaviour of the mean field attenuation coefficient and we shall show that, for appropriate models of the random velocity fluctuation, the mean field approximation could also provide a frequency-dependence of Q^{-1} that is compatible with AKI's data.

2. General theorem on the asymptotic behaviour of the mean wave attenuation coefficient

Suppose an elastic wave u is propagating in a medium with the random velocity distribution

$$c(\mathbf{x}) = c_0 + a\varepsilon(\mathbf{x}) + b\varepsilon^2(\mathbf{x}) + O(\varepsilon^3) \tag{2}$$

where, letting square brackets denote expectations and using the terminology of TATARSKI [1967], $\varepsilon(\mathbf{x})$ is a homogeneous isotropic random field with $<\varepsilon(\mathbf{x})> = 0, <\varepsilon^2(\mathbf{x})> = \varepsilon^2$. If we introduce the average wave number $k_0 = \omega/c_0$ the wave equation

$$\Delta u + \frac{\omega^2}{c^2}u = 0 \tag{3}$$

can be developed in series in terms of powers of $\varepsilon(\mathbf{x})$:

$$\Delta u(\mathbf{x}) + k_0^2 [1 + \gamma_1 \varepsilon(\mathbf{x}) + \gamma_2 \varepsilon^2(\mathbf{x})] u(\mathbf{x}) = 0 \tag{4}$$

where terms of $O(\varepsilon^3)$ had been omitted.

In terms of the coefficients a and b of Eq. (2) the constants γ_1 and γ_2 can be expressed as

$$\gamma_1 = -\frac{2a}{c_0} \qquad \gamma_2 = \frac{3a^2}{c_0^2} - \frac{2b}{c_0} \tag{5}$$

It should be noted that for the most conventional random wave propagation problems the general expression (2) of the velocity distribution assumes one of the following forms:

$$c_1(\mathbf{x}) = c_0(\mathbf{x}) + \varepsilon(\mathbf{x}) \tag{6a}$$

$$c_2(\mathbf{x}) = c_0(\mathbf{x}) [1 + \varepsilon(\mathbf{x})] = c_0(\mathbf{x}) + c_0(\mathbf{x})\varepsilon(\mathbf{x}) \tag{6b}$$

$$c_3(\mathbf{x}) = \frac{c_0(\mathbf{x})}{1 + \varepsilon(\mathbf{x})} = c_0(\mathbf{x}) - c_0(\mathbf{x})\varepsilon(\mathbf{x}) + c_0(\mathbf{x})\varepsilon^2(\mathbf{x}) + O(\varepsilon^3) \tag{6c}$$

The form (6c) is widely used in the perturbation solution of the random wave equation [KELLER 1964, KARAL–KELLER 1964]; propagation problems in turbulent atmospheres [TATARSKI 1967] are generally solved on the basis of model (6b); for seismic problems expression (6a) seems to be the most appropriate [KATS et al. 1969, KORVIN 1973]. Since, by introducing a new variable $\varepsilon' = \varepsilon/c_0$ model (6a) can be reduced to (6b), the case (6a) should not be dealt with separately.

Matching Eqs. (6b, 6c), in turn, with the general expression (2), the coefficients a, b become

$$a(\mathbf{x}) = c_0(\mathbf{x}) \qquad b(\mathbf{x}) = 0 \tag{7b}$$

$$a(\mathbf{x}) = -c_0(\mathbf{x}) \qquad b(\mathbf{x}) = c_0(\mathbf{x}) \tag{7c}$$

that is, by Eq. (5), the coefficients γ_1 and γ_2 of the wave equation (4) become for the respective velocity models (6b), (6c):

$$\gamma_1 = -2 \qquad \gamma_2 = 3 \tag{8b}$$

$$\gamma_1 = +2 \qquad \gamma_2 = 1 \tag{8c}$$

Let us introduce the normalized random variable

$$\mu(\mathbf{x}) = \frac{\varepsilon(\mathbf{x})}{<\varepsilon^2(x)>^{1/2}} = \frac{\varepsilon(\mathbf{x})}{\varepsilon} \tag{9}$$

and denote by $N(r)$ the autocorrelation function of $\mu(x)$:

$$<\mu(\mathbf{x})\mu(\mathbf{x}')> = N(r), \qquad r = |\mathbf{x} - \mathbf{x}'| \tag{10}$$

If we expect a planar wave solution to Eq. (4) as

$$<u(\mathbf{x})> = A e^{ikx} \tag{11}$$

for the mean field $<u(\mathbf{x})>$ it can be shown by a slight generalization [KORVIN 1977] of KELLER's stochastic perturbation method [KELLER 1964, KARAL–KELLER 1964] that the effective wave number k satisfies a dispersion relation

$$k^2 = k_0^2 + \varepsilon^2 \gamma_2 k_0^2 + \varepsilon^2 \frac{k_0^4}{k} \gamma_1^2 \int_0^\infty e^{ik_0 r} \sin kr N(r) \, dr \tag{12}$$

For low frequencies the dispersion relation (12) can be solved by the method of successive approximations:

$$\frac{k^2}{k_0^2} \approx 1 + \varepsilon^2 \gamma_2 + \varepsilon^2 k_0 \gamma_1^2 \int_0^\infty e^{ik_0 r} \sin k_0 r N(r)\, dr =$$

$$= 1 + \varepsilon^2 \gamma_2 + \varepsilon^2 k_0 \gamma_1^2 \frac{i}{2} \int_0^\infty (1 - e^{2ik_0 r}) N(r)\, dr \tag{13}$$

from where the effective absorption coefficient, i.e. the imaginary part of the effective wave number, becomes

$$a = \frac{\varepsilon^2 \gamma_1^2}{4} k_0^2 \int_0^\infty (1 - \cos 2k_0 r) N(r)\, dr \tag{14}$$

For exponential autocorrelation functions Eq. (14) provides the well-known Rayleigh scattering on the small-scale inhomogeneities [KARAL–KELLER 1964, KORVIN 1977].

In what follows we shall show that the successive approximation solution to Eq. (12) cannot be justified for higher frequencies, that is — in contradistinction to the statement of SATO [1982 a, b] and WU [1982] — the mean field approximation does not imply a scattering that would infinitely increase with frequency.

Indeed, if we write Eq. (13) as

$$\frac{k^2}{k_0^2} = 1 + \varepsilon^2 \gamma_2 + \varepsilon^2 k_0 \gamma_1^2 \frac{i}{2} \int_0^\infty N(r)\, dr - \varepsilon^2 k_0 \gamma_1^2 \frac{i}{2} \int_0^\infty e^{2ik_0 r} N(r)\, dr \tag{15}$$

the second integral on the r.h.s. of Eq. (15) behaves, by Riemann's lemma, asymptotically as

$$\int_0^\infty e^{2ik_0 r} N(r)\, dr = O\left(\frac{1}{k_0}\right) \quad \text{if } k_0 \to \infty \tag{16}$$

that is, if

$$\int_0^\infty N(r)\, dr \neq 0 \tag{17}$$

the successive approximation would imply

$$\frac{k^2}{k_0^2} \to \infty \quad \text{if } k_0 \to \infty \tag{18}$$

that would contradict the principle of causality [cf. AZIMI et al. 1968, CLAER-BOUT 1976]. This contradiction shows that for $k_0 \gg 1$ the dispersion relation (12) should be solved more accurately.

The solution of Eq. (12) for $k_0 \gg 1$ will be sought for in the form

$$k = k_0 \left(\kappa_1 + i \frac{\kappa_2}{k_0} \right) \tag{19}$$

where $\kappa_1(k_0)$ and $\kappa_2(k_0)$ are real functions of the average wave number and, by the principle of causality, we assume that

$$\lim_{k_0 \to \infty} \frac{\kappa_2(k_0)}{k_0} = 0 \tag{20}$$

Since in the high-frequency approximation the inhomogeneities $\varepsilon(x)$ satisfying Eq. (2) always reduce the effective propagation speed [see KORVIN 1973], we also have

$$\kappa_1(k_0) \geqq 1 \quad \text{for} \quad k_0 \gg 1 \tag{21}$$

The integral on the r.h.s. of Eq. (12) can be written as

$$I(k_1, k_2) = \int_0^\infty e^{ik_0 r} \sin kr N(r) \, dr =$$
$$= \frac{1}{2i} \int_0^\infty e^{i(k+k_0)r} N(r) \, dr - \frac{1}{2i} \int_0^\infty e^{i(k-k_0)r} N(r) \, dr \tag{22}$$

where, because of Eq. (21),

$$Re\,(k + k_0) > 0, \quad Re\,(k - k_0) \geqq 0 \tag{23}$$

For the determination of the asymptotic behaviour of the integrals figuring in Eq. (22) we shall make use of the following general theorem [see ERDELYI 1956, p. 47]:

If $\Phi(t)$ is N times continuously differentiable for $a \leqq t \leqq b$ then

$$\int_a^b e^{ixt} \Phi(t) \, dt = B_N(x) - A_N(x) + o(x^{-N}) \quad \text{as} \quad x \to \infty \tag{24}$$

where

$$A_N(x) = \sum_{n=0}^{N-1} i^{n-1} \Phi^{(n)}(a) x^{-n-1} e^{ixa}$$

$$B_N(x) = \sum_{n=0}^{N-1} i^{n-1} \Phi^{(n)}(b) x^{-n-1} e^{ixb}$$

and

$$\Phi^{(n)} = d^n \Phi / dt^n.$$

The result remains true when $a = -\infty$ *(or* $b = \infty$*) provided that* $\Phi^{(n)}(t) \to 0$ *as* $t \to -\infty$ *(or* $t \to \infty$*) for each* $n = 0, 1, \ldots, N-1$, *and provided further that* $\Phi^{(n)}(t)$ *is integrable over* (a, b).

Equation (24) can readily be derived by repeated partial integrations, the remainder term is obtained by Riemann's lemma.

By Eq. (24) the integral expression (22) becomes, with an accuracy of $o(k_0^{-2})$ and by taking into account that $N(0) = 1$ (cf. Eqs. 9 and 10):

$$I(k_1, k_0) = \frac{1}{2i} \left\{ \frac{1}{i(k_0+k)} \left(1 - \frac{N'(+0)}{i(k_0+k)}\right) + \right.$$

$$\left. + \frac{1}{i(k_0-k)} \left(1 - \frac{N'(+0)}{i(k_0-k)}\right) \right\} + O\left(\frac{1}{k_0^3}\right) =$$

$$= -\frac{i}{2} \left\{ \frac{1}{-N'(+0) - ik_0 - ik} - \frac{1}{-N'(+0) - ik_0 + ik} \right\} + O\left(\frac{1}{k_0^3}\right)$$

that is, from Eq. (12):

$$k^2 = k_0^2 + \varepsilon^2 \gamma_2 k_0^2 - \varepsilon^2 \frac{k_0^4}{k} \gamma_1^2 \frac{i}{2} \times$$

$$\times \left[\frac{1}{-N'(+0) - ik_0 - ik} - \frac{1}{-N'(+0) - ik_0 + ik} \right] + O(\varepsilon^2) \qquad (25)$$

If $N'(+0) \neq 0$ then, for sufficiently large values of

$$k_0/|N'(+0)| \text{ (if } k_0/|N'(+0)| \gg 1/\varepsilon)$$

the solution of Eq. (25) becomes

$$k = k_0 \left(1 + \delta_1 <\varepsilon^2>^{1/2} + \delta_2 <\varepsilon^2> - \frac{i\delta_3}{2k_0} N'(+0) + O(\varepsilon^2)\right) \qquad (26a)$$

where the coefficients δ_i are related to the $\gamma_i - s$ (of Eqs. 4, 5, 8) by

$$\delta_1 = \frac{|\gamma_1|}{2} \qquad (26b)$$

$$\delta_2 = \left\{ \frac{\gamma_1^2}{4} - \gamma_2 \right\} \qquad (26c)$$

$$\delta_3 = 1 \qquad (26d)$$

Equation (26a) shows that, if $N'(+0) \neq 0$, for high frequencies the imaginary part of k, that is the effective mean field attenuation coefficient, tends to a frequency-independent constant value

$$a(k_0) \to -\frac{1}{2} N'(+0) \text{ if } \frac{k_0}{|N'(+0)|} \to \infty \tag{27}$$

Since, because of the Cauchy-Schwartz inequality $N(r) \leq N(0)$ for $r \neq 0$, the absorption coefficient given by Eq. (27) is always positive. Also, observe that the high-frequency mean wave absorption coefficient is independent of ε and of the coefficients γ_1 and γ_2, that is of the actual strength of the inhomogeneities, and it only depends on the local geometry of their distribution, expressed by $N'(+0)$.

In the particular case of the velocity distribution (6c), and for the correlation function $N(r) = \exp(-r/a)$, Eq. (27) reduces to $a(k_0) = \frac{1}{2a}$ (if $ak_0 \gg <\varepsilon^2>^{-1/2}$) previously derived by KARAL–KELLER [1964, Eq. 31].

If $N'(+0) = 0$, the mean wave absorption coefficient tends to zero at least as fast as $O(1/k_0)$. It should be noted that the essential difference between the attenuating properties of random media for which $N'(+0) \neq 0$ and $N'(+0) = 0$, respectively, has also been observed — in another context — in a discussion between ARMSTRONG and the present author in 1981 [KORVIN 1981].

3. Application of the general theorem to AKI's shear wave absorption data

On the basis of the general result of Eq. (27) a possible explanation for AKI's [1980] shear wave absorption data could be provided by the following random velocity model: Suppose the shear wave velocities $c(\mathbf{x})$ are distributed in the regions studied as

$$c(\mathbf{x}) = c_0 + \varepsilon(\mathbf{x}) = c_0 \left(1 + \frac{\varepsilon(\mathbf{x})}{c_0}\right) \tag{28}$$

where the fluctuating part of the velocity is composed of a "slowly" varying part $\varepsilon_1(\mathbf{x})$ of relatively larger scatter and of a "rapidly" varying part $\varepsilon_2(\mathbf{x})$ of smaller scatter; suppose, further, that both ε_1 and ε_2 are of zero expectance, that ε_1 and ε_2 are independent, and that both fluctuations have a depth dependence that is basically Poisson in character [as suggested, e.g., in KATS et al. 1969, TUCHOLKE 1980]:

$$\varepsilon(\mathbf{x}) = \varepsilon_1(\mathbf{x}) + \varepsilon_2(\mathbf{x}) \tag{29a}$$

$$<\varepsilon_1(\mathbf{x})> = <\varepsilon_2(\mathbf{x})> = 0 \tag{29b}$$

$$<\varepsilon_1^2(\mathbf{x})> = \varepsilon_1^2 \qquad <\varepsilon_2^2(\mathbf{x})> = \varepsilon_2^2 \tag{29c}$$

$$\langle\varepsilon_1(\mathbf{x})\varepsilon_2(\mathbf{x'})\rangle = 0 \quad \text{for all } \mathbf{x}, \mathbf{x'} \tag{29d}$$

$$\langle\varepsilon_1(\mathbf{x})\varepsilon_1(\mathbf{x'})\rangle = \varepsilon_1^2 \exp(-r/r_1) \tag{29e}$$

$$\langle\varepsilon_2(\mathbf{x})\varepsilon_2(\mathbf{x'})\rangle = \varepsilon_2^2 \exp(-r/r_2) \tag{29f}$$

$$\varepsilon_1^2 \gg \varepsilon_2^2 \tag{29g}$$

$$r_1 \gg r_2 \tag{29h}$$

where in Eqs. (29e and f) $r = |\mathbf{x} - \mathbf{x'}|$. From Eqs. (9, 10, 29a—f) we have

$$N(r) = \frac{1}{\varepsilon_1^2 + \varepsilon_2^2} [\varepsilon_1^2 e^{-r/r_1} + \varepsilon_2^2 e^{-r/r_2}] \tag{30}$$

For low frequencies, by Eqs. (28), (7b), (8b), (14), (29a, b, c) and (30), we have

$$a = \frac{k_0^4}{c_0^2} (\varepsilon_1^2 r_1^3 + \varepsilon_2^2 r_2^3) \tag{31}$$

that is, we get the conventional Rayleigh scattering from both kinds of inhomogeneities ε_1 and ε_2.

For higher frequencies, by strength of the general theorem (27) we have, for the correlation function (30):

$$a \sim -\frac{1}{2} N'(+0) = \frac{1}{2} \frac{1}{\varepsilon_1^2 + \varepsilon_2^2} \left[\frac{\varepsilon_1^2}{r_1} + \frac{\varepsilon_2^2}{r_2}\right] \tag{32}$$

If we define the mean correlation length $\bar{r}$ by

$$\frac{1}{\bar{r}} = \frac{1}{\varepsilon_1^2 + \varepsilon_2^2} \left[\frac{\varepsilon_1^2}{r_1} + \frac{\varepsilon_2^2}{r_2}\right]$$

the asymptotic expression (32) is valid if

$$k_0\bar{r} \gg 1.$$

If we make a further assumption, that

$$\frac{\varepsilon_2^2}{\varepsilon_1^2} \gg \frac{r_2}{r_1} \tag{29i}$$

Eq. (32) can be approximated by

$$a \sim \frac{1}{2} \frac{\varepsilon_2^2}{\varepsilon_1^2} \frac{1}{r_2} \tag{33}$$

Matching this expression with DAINTY's result for the scattering part of Q^{-1} (cf. Eq. 1) and recalling that

$$\frac{c_0 a}{f\pi} = \frac{1}{Q} \qquad (34)$$

we have

$$r_2 = \frac{\varepsilon_2^2}{\varepsilon_1^2} \cdot g_0^{-1} \qquad (35)$$

where $g_0^{-1} = 100$ km for AKI's Japan data [DAINTY 1981]. On the other hand the Rayleigh-scattering result seems to be valid up to frequencies of about 0.3–0.4 Hz, that is r_2 is less than or equal to the wavelength corresponding to these frequencies:

$$r_2 \leqq 10 \div 12 \text{ km} \qquad (36)$$

If we take the correlation distance r_2 of the short-distance inhomogeneities as

$$r_2 \approx 10 \div 12 \text{ km}$$

in accordance with earlier results of AKI [1973] and CAPON [1974], the random velocity model (28) subject to the constraints (29a)–(29i) can be satisfied, for example, by the following choice of parameters:

$r_2 \approx 10 \div 12$ km   [cf. Eq. (36); AKI 1973, CAPON 1974]
$\varepsilon_2/c_0 \approx 2 \div 4\%$ [cf. CAPON 1974]
$\left(\dfrac{\varepsilon_2}{c_1} \Big/ \dfrac{\varepsilon_1}{c_1}\right)^2 = r_2 g_0 \approx 10 \cdot 0.01 = 0.1$ [cf. Eq. (35) and DAINTY 1981], that is,

$$\frac{\varepsilon_1}{c_0} \approx 3 \cdot \frac{\varepsilon_2}{c_0} \approx 6 \div 12\%$$

and finally, from Eq. (29i)

$$r_1 \gg r_2 \cdot \frac{\varepsilon_1^2}{\varepsilon_2^2} \approx 10 r_2$$

that is $r_1 > 100 \div 120$ km. (It is easy to check that $k_0 \bar{r} \gg 1$ even for 1 Hz.)

Thus, we have shown that for a plausible choice of the random velocity fluctuations a mean wave attenuation theory can, in principle, also explain the observed frequency dependence of Q^{-1}, in contradistinction to the statement of WU [1982] and SATO [1982a, 1982b].

REFERENCES

AKI, K. 1973: Scattering of P-waves under the Montana LASA. J. Geoph. Res. **78**, 8, pp. 1334–1346

AKI, K. 1980: Attenuation of shear waves in the lithosphere for frequencies from 0.05 to 25 Hz. Phys. Earth. Planet. Int. **21**, 1, pp. 50–60

AKI, K. 1981: Scattering and attenuation of high-frequency body waves (1–25 Hz) in the lithosphere. Phys. Earth. Planet. Int. **26**, 4, pp. 241–243

ATTEWELL, P. B., RAMANA, Y. W. 1966: Wave attenuation and internal friction as functions of frequency in rocks. Geophysics, **31**, 6, pp. 1049–1056

AUBERGER, M., RINEHART, J. S. 1961: Ultrasonic velocity and attenuation of longitudinal waves in rocks. J. Geoph. Res. **66**, 1, pp. 191–199

AZIMI, SH. A., KALININ, A. V., KALININ, V. V., PIVOVAROV, B. L. 1968: Impulse and transient characteristics of media with linear and quadratic absorption laws (in Russian). Izv. AN SSSR Fiz. Zemli, 2, pp. 42–54

BODOKY, T., KORVIN, G., LIPTAI, I., SIPOS, J. 1971: An analysis of the initial seismic pulse near underground explosions. Geoph. Trans. **20**, 3–4, pp. 7–27

BRADLEY, J. J., FORT, A. N. JR. 1966: Internal friction in rocks. In: Handbook of Physical Constants (Ed. Clark, S. P. Jr). Geol. Soc. Am. Memoir, 97, pp. 175–193

CAPON, J. 1974: Characterization of crust and upper mantle structure under LASA as a random medium. Bull. Seism. Soc. Am. **64**, 1, pp. 235–266

CLAERBOUT, J. F. 1976: Fundamentals of geophysical data processing. McGraw-Hill Book Co., New York

CROWE, C., ALHILALI, K. 1975: Attenuation of seismic reflections as a key to lithology and pore filler. 60th Annual Mtg. AAPG April 7–9, Dallas

DAINTY, A. M. 1981: A scattering model to explain seismic Q observations in the lithosphere between 1 and 30 Hz. Geoph. Res. Letters, **8**, 11, pp. 1126–1128

ERDELYI, A. 1956: Asymptotic expansions. Dover Publ. Inc., New York

FEDOTOV, S. A., BOLDYREV, S. A. 1969: On the dependence of the body wave absorption from the frequency in the crust and upper mantle of the Kurile archipelago (in Russian). Izv. AN SSSR Fiz. Zemli, 9, pp. 17–33

KARAL, F. C. JR., KELLER, J. B. 1964: Elastic, electromagnetic, and other waves in a random medium. J. Math. Phys. **5**, 4, pp. 537–549

KATS, S. A., KONDRATOVICH, YU. V., ISAEV, V. S., VILKOVA, E. S. 1969: The effect of the random structure of a set of layers on the dynamic properties of the reflected waves (in Russian). Prikl. Geofizika, 57, pp. 70–80

KELLER, J. B. 1964: Stochastic equations and wave propagation in random media. Proc. Symp. Appl. Math. **16**, pp. 145–170

KIKUCHI, M. 1981: Dispersion and attenuation of elastic waves due to multiple scattering from cracks. Phys. Earth Planet. Int. **27**, 2, pp. 100–105

KNOPOFF, L. 1964: Q. Rev. Geoph. **2**, 4, pp. 625–660

KORVIN, G. 1973: Certain problems of seismic and ultrasonic wave propagation in a medium with inhomogeneities of random distribution. Geoph. Trans. **21**, 1–4, pp. 5–34

KORVIN, G. 1977: Certain problems of seismic and ultrasonic wave propagation in a medium with inhomogeneities of random distribution. II. Wave attenuation and scattering on random inhomogeneities. Geoph. Trans. **24**, Suppl. 2, pp. 3–38

KORVIN, G. 1980: The effect of random porosity on elastic wave attenuation. Geoph. Trans. **26**, pp. 43–56

KORVIN, G. 1981: Discussion on: "Frequency-independent background internal friction in heterogeneous solids" (Armstrong, B. H. 1980: Geophysics, **45**, 6, pp. 1042–1054) with Author's reply. Geophysics, **46**, 9, pp. 1314–1315

LEE, W. B., SOLOMON, S. C. 1978: Simultaneous inversion of surface wave phase velocity and attenuation: Love waves in Western North America. J. Geoph. Res. **83**, pp. 3389–3400

MILITZER, H., SCHÖN, J. 1972: Some theoretical and experimental results for the determination of characteristic properties of naturally bedded rocks on the basis of seismic measurements. 24th International Geology Congress, Montreal, Canada, Section 9, pp. 158–164

Militzer, H., Stoll, R. 1968: Vibratorseismische Messungen in situ zur Bestimmung eines frequenzabhängigen Absorptionskoeffizienten. Bergakademie, **20**, 9, pp. 518–521

Nur, A. 1971: Viscous phase in rocks and the low-velocity zone. J. Geoph. Res. **76**, 5, pp. 1270–1278

Petrovics, I., Jánvári, J., Korvin, G., Sipos, J. 1975: Investigation of the correlation of reflecting horizons via digital filtering and energy analysis (in Hungarian). Magyar Geofizika, **16**, 3, pp. 98–105

Rautian, T. G., Khalturin, V. I. 1978: The use of the Coda for determination of the earthquake source spectrum. Bull. Seismol. Soc. Am. **68**, 4, pp. 923–948

Sato, H. 1982a: Amplitude attenuation of impulsive waves in random media based on travel time corrected mean wave formalism. J. Acoustic Soc. Am. **71**, 3, pp. 559–564

Sato, H. 1982b: Attenuation of S-waves in the lithosphere due to scattering by its random velocity structure. J. Geoph. Res. **87**, pp. 7779–7785

Solomon, S. C. 1972: Seismic wave attenuation and partial melting in the upper mantle of North America. J. Geoph. Res. **77**, 8, pp. 1483–1502

Tatarski, V. I. 1967: Wave propagation in a turbulent medium. Dover Publ., Inc. New York

Tsai, Y. B., Aki, K. 1969: Simultaneous determination of seismic moment and attenuation of seismic surface waves. Bull. Seismol. Soc. Am. **59**, 1, pp. 275–287

Tucholke, B. E. 1980: Acoustic environment of the Hatteras and Nares Abyssal Plains, Western North Atlantic Ocean, determined from velocities and physical properties of sediment cores. J. Acoustic Soc. Am. **68**, 5, pp. 1376–1390

Warren, N. 1972: Q and structure. The Moon, **4**, pp. 430–441

Wu, Ru-Shan 1982: Attenuation of short period seismic waves due to scattering. Geophys. Res. Letters 9, 1, pp. 9–12

KORVIN GÁBOR

ÁLTALÁNOS TÉTEL AZ ÁTLAGOS HULLÁMTÉR CSILLAPODÁSÁRÓL

1980-ban Aki meggyőzően bizonyította, hogy a földkéregben és a köpenyben terjedő S hullámokra a Q minőségi tényező az 1—25 Hz tartományban a frekvencia növekedő függvénye, ellentétben a Q állandóságát kimondó korábbi feltevésekkel és elméletekkel. A dolgozatban megmutatjuk, hogy a jelenség megmagyarázható a véletlen hullámterjedés „átlagos tér" elméletének keretein belül. Általános érvényű aszimptotikus összefüggést vezetünk le az átlagos tér csillapodási együtthatójának nagyfrekvenciás viselkedésére. Az összefüggés alkalmazásaként megmutatjuk, hogy — fizikailag reális véletlen sebesség fluktuációkat feltételezve — az átlagos tér közelítés Aki adataival összemérhető $Q(f)$ függést szolgáltat.

Г. КОРВИН

ОБЩЕЕ ПОЛОЖЕНИЕ О ЗАТУХАНИИ СРЕДНЕГО ПОЛЯ ВОЛН

В 1980 г. Аки убедительно доказал, что для распространяющихся в земной коре и мантии волн типа S качественный фактор Q возрастает с частотой в диапазона от 1 до 25 Гц, в противоположность прежним предположениям и теориям, высказывающим постоянство Q. В работе показано, что явление может быть объяснено в рамках теории «среднего поля» случайного распространения волн. Выводится асимптотическая зависимость, имеющая всеобщее действие, для высокочастотного поведения коэффициента затухания среднего поля. В качестве применения зависимости показывается, что при предположении физически обоснованных случайных колебаний скорости аппроксимация при помощи среднего поля дает функцию $Q(f)$, соизмеримую с данными Аки.

RELATIONSHIP BETWEEN LONGITUDINAL WAVE VELOCITY AND DENSITY IN SEDIMENTARY SERIES

G. N. GOGONENKOV*, YU. V. KRASAVIN*

In order to develop criteria for interpreting the curves obtained by the pseudo-acoustic transformation of seismic traces the paper analyses the results of sonic and gamma-gamma logs measured in wells in the Ural–Volga region, in the Caucasian Foredeeps and in W. Siberia. The coefficients of the velocity- and density variations are computed and the correlation between these parameters is analysed.

It is shown that the degree of correlation between velocity and density strongly depends on the lithology of the formation and this should be taken into account in the inversion of the seismic traces.

d: velocity, density, pseudo-acoustic log, lithology

1. Introduction

In the last few years considerable attention has been paid to the transformation of seismic traces into acoustic impendance logs (pseudo-acoustic logs, cf. GOGONENKOV et al. 1980, LAVERGNE et al. 1977). One of the most important steps in this transformation is the computation of the scaling factor and the determination of the proper polarity by means of comparing the seismic data with the acoustic impedance (i.e. the product of the longitudinal wave velocity and the density) directly measured in boreholes. Comparison of the pseudo-acoustic log (PAL) with the directly measured acoustic impedances is of basic importance in estimating the reliability of the results of the PAL transform, and for their geological interpretation.'Unfortunately, in most cases no velocity- or density logs are available for this comparison.

The properties of the detailed density distribution $\rho(z, x, y)$ in naturally bedded sedimentary formations have been much less studied than the distribution characteristics of the longitudinal velocity. Since the solution of the inverse dynamic problem yields the product of these quantities, it is of utmost importance to establish a connection between V and ρ in actual sections.

The relationship between V and ρ has been analysed in a number of previous studies (BEREZKIN 1963, MIHAILOV 1965, GOGONENKOV 1972, GARDNER et al. 1974). In GOGONENKOV (1972) a quantitative estimation is given for the correlation relationship between V and ρ, based on the data of G. I. PETKEVICH from the Carpathian Foredeep, of E. K. ELANSKAYA from the Kuibishev–Volga region, and V. F. KODYARM from Bashkiria. It is shown that the V–ρ relationship can be approximated fairly well by the law

* Central Geophysical Expedition of the Oil Ministry, 123298 Moscow, ul. Narodnogo Opolcheniya 40, korp. 3, USSR

$$\rho = m \cdot V^n \tag{1}$$

where m varies from 0.293 to 0.302 for the different regions, n varies between 0.134 and 0.268.

GARDNER et al. (1974) compiled a number of $V–\rho$ relationships for rocks of different lithologies. It is shown that for the basic lithologic types (sandstones, shales, limestones and dolomites) the $V–\rho$ relationship is sufficiently well described by Eq. (1). The hydrochemical sediments, however, i.e. salt, gypsum, anhydrite and also coal, are characterized by an anomalous relationship between V and ρ (Fig. 1.). All the data presented in GOGONENKOV (1972), BEREZKIN (1963), MIKHAILOV (1965) and GARDNER et al. (1974) are based on investigations carried out on core samples. There are much fewer data available on in situ velocity–density studies — even though such data were of basic importance in the interpretation of seismic materials. The development of the gamma–gamma density log (GGDL, cf. GULIN 1975) has created novel possibilities for the experimental study of the $V–\rho$ relationship in real media. First of all, let us call attention to the important contribution of AROV (1981) who, on the basis of a limited amount of data, compared the in situ measured densities in real deposits with those values measured in saturated core samples. It was found that the deviations between the different measurements did not exceed 0.02 g/cm³.
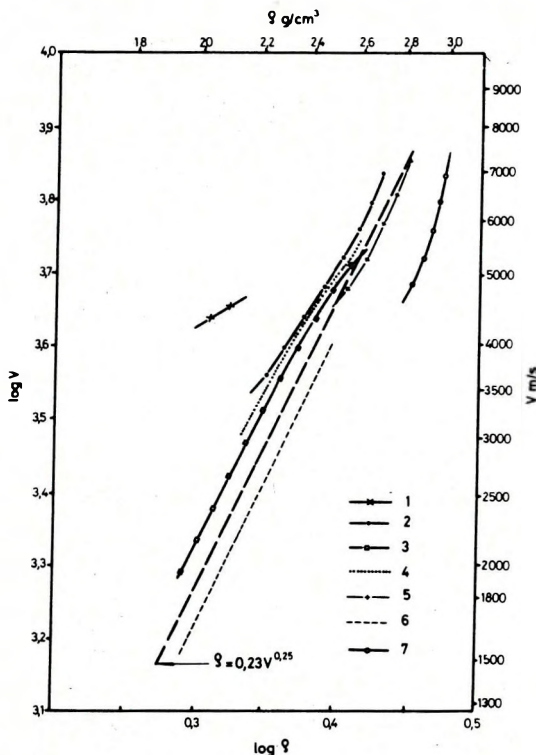
Fig. 1. Connection between velocity and density for different types of rocks (after GREGORY 1977)
1 — rock salt; 2 — limestone; 3 — sandstone; 4 — time average (sandstone); 5 — dolomite; 6 — shale; 7 — anhydrite

1. ábra. A sebesség és sűrűség közti összefüggés különböző kőzettípusok esetében (GREGORY 1977 szerint)
1 — kősó; 2 — mészkő; 3 — homokkő; 4 — homokkő idő átlaga; 5 — dolomit; 6 — pala; 7 — anhidrit

Рис. 1. Зависимость скорости от плотности для различных типов пород (по ГРЕГОРИ 1977)
1 — кам. соль; 2 — известняк; 3 — песчаник; 4 — среднее время (песчаник); 5 — доломит; 6 — глина; 7 — ангидрит

In Japan, ISHII et al. (1975) also reported on the relationship between V and ρ, obtained from acoustic logs and GGDL data. Their data are also fitted by a law of the form of Eq. (1); in some parts of the section there is a very good correlation between V and ρ, in other parts the correlation deteriorates — though the paper does not provide any explanation for these discrepancies.

In the present paper an alaysis of sonic log and GGDL data will be given obtained from the Ural–Volga region, from the Caucasian Foredeeps and from West Siberia. Before describing the methods and results, let us briefly discuss the most important parameters in the V–ρ relationship from the point of view of the seismic method.

2. Statistical estimation of the contribution of the velocities and of the densities to the distribution of the coefficient of reflection

Let us suppose that for a sedimentary series the values of V and ρ in the layers follow a normal distribution P:

$$P(V) = \frac{1}{\sigma_V \sqrt{2\pi}} \cdot e^{-(V - V_0)^2 / 2\sigma_V^2}$$

$$P(\rho) = \frac{1}{\sigma_\rho \sqrt{2\pi}} \cdot e^{-(\rho - \rho_0)^2 / 2\sigma_\rho^2}$$

(2)

where V_0 and ρ_0 are the mathematical expectations, σ_V^2 and σ_ρ^2 are the dispersions of V and ρ, respectively. If the acoustic impedance is given by $W = V \cdot \rho$ and the correlation between V and ρ is characterized by the correlation coefficient R, W will be distributed according to the law

$$R(W) = \frac{1}{\sigma_W \sqrt{2\pi}} \cdot e^{-(W - W_0)^2 / 2\sigma_W^2}$$

(3)

where $W_0 = \rho_0 V_0$ (4)

$$\sigma_W^2 = \rho_0^2 \sigma_V^2 + 2R\rho_0 V_0 \sigma_\rho \sigma_V + V_0^2 \sigma_\rho^2$$

(5)

Let us introduce the reflection coefficient (K) for the case of normally incident waves at the boundary of two layers i and j:

$$K_{ij} = \frac{W_j - W_i}{W_j + W_i}$$

(6)

let us apply the transformation described in VELZEBOER (1981). Suppose that the first two momenta of W_i and W_j are equal and that W_i and W_j are uncorrelated.

Under these assumptions we obtain

$$K_0(i, j) = 0 \qquad \sigma_K(i, j) = \frac{1}{\sqrt{2}} \cdot \frac{\sigma_W}{W_0} \tag{7}$$

where $K_0(i, j)$ and $\sigma_K(i, j)$, respectively, are the expectance and dispersion of the coefficient of reflection. Substituting Eqs. (3) and (4) into (7) and omitting the indices i and j, we obtain

$$\sigma_K = \frac{1}{\sqrt{2}} \left(\frac{\sigma_V^2}{V_0^2} + 2R \frac{\sigma_V}{V_0} \cdot \frac{\sigma_\rho}{\rho} + \frac{\sigma_\rho^2}{\rho_0^2} \right)^{1/2} \tag{8}$$

Thus, the standard deviation of the reflection coefficient can be expressed in the above-described model — in accordance with the earlier statistical experimental findings in AGARD 1961, BOIS and HEMON, 1963, GOGONENKOV and ASRIYANTS 1969 — in terms of the coefficients of variation $\left(\frac{\sigma_x}{x_0} \right)$ of the velocity and the density, and of their correlation coefficient.

In the case of a complete positive correlation between V and ρ, that is, for $R = +1$:

$$\sigma_K = \frac{1}{\sqrt{2}} \left(\frac{\sigma_V}{V_0} + \frac{\sigma_\rho}{\rho_0} \right), \tag{9}$$

for an inverse correlation, i.e. for $R = -1$:

$$\sigma_K = \frac{1}{\sqrt{2}} \left(\frac{\sigma_V}{V_0} - \frac{\sigma_\rho}{\rho_0} \right), \tag{10}$$

while in the absence of any correlation ($R = 0$):

$$\sigma_K = \frac{1}{\sqrt{2}} \left(\frac{\sigma_V^2}{V_0^2} + \frac{\sigma_\rho^2}{\rho_0^2} \right)^{1/2}. \tag{11}$$

This analysis has shown that for a proper interpretation of the estimated acoustic impedance values one has to know the variation coefficients of V and ρ, and the character of the correlation between these parameters.

3. Characteristics of the experimental data and method of their analysis

The coefficients of the velocity- and density variation and the correlation coefficient R were estimated on the basis of measured sonic logs (SL) and gamma-gamma logs (GGL) from 9 wells. Study sites and depth ranges are

compiled in *Table I.* The depth ranges studied include some of the most promising hydrocarbon deposits. The premliminary sonic- and gamma-gamma logs had been checked and edited in order to eliminate gross errors due to cavities or other effects (GULIN 1975), making use of caliper logs and other kinds of standard well logs. The velocity from the sonic log had been estimated from the t_1, t_2 and Δt curves; recorded acoustic full waveforms had also been utilized.

Next, on the basis of a joint analysis of the $V(z)$ and $\rho(z)$ curves the intervals studied were divided to homogeneous layers of 3–15 m thickness. Each of these layers was then represented by the mean value of the respective parameters within the layer. The values of V and ρ computed for the subsequent layers are shown in *Figs. 2,* and *3* for typical wells.

The values of V and ρ were fitted by two kinds of correlation laws. The first is a traditional one, similar to that applied in GOGONENKOV 1972, GARDNER et al. 1974, ISHII et al. 1975, where the principal aim is to find some quantitative relationship in order to predict one of the parameters from the values of the other. Let us refer to this law as "general correlation". It can be estimated from plots where one of the axes denotes the values of velocities, the other the densities, in the same layer. Typical plots are shown in *Fig. 4.* (a, b) for several well and for all layers belonging to the given lithology.

Another kind of correlation law, of particular significance for the analysis of seismic data, establishes the correlation between the $V(z)$ and $\rho(z)$ curves. This type of correlation will be called "correlation versus depth"—R_z. Strictly speaking, this type of correlation coefficient R_z should be used in formulae (9)–(11). In order to exclude the effect of the different gradients of the $V(z)$ and $\rho(z)$ curves, and to determine the peculiarities of the correlation between V and ρ in the different layers, the estimation of R_z has been realized in subsequent intervals of 400–500 m thickness (cf. *Table I.*) according to the formula

$$R_z = \frac{\sum\limits_{i}^{j}(V_i - \overline{V})\cdot(\rho_i - \overline{\rho})}{\sqrt{\sum\limits_{i}^{j}(V_i - V)^2 \cdot \sum\limits_{i}^{j}(\rho_i - \rho)^2}}, \tag{12}$$

where i is the serial number of the layers in the given interval ($i = 1, 2, \ldots, j$).

4. Results

The basic quantitative estimations of the characteristics of the correlations, and of the velocities and densities, respectively, are compiled in Table I. Consider first the coefficients of the variations of V and ρ. As seen from the Table, the mean values and standard deviations of the investigated parameters follow the well-known rules: the mean values increase with increasing depth of the ranges analysed, and with increasing values of the carbonate fraction.

The standard deviation of the velocity, σ_V, is the more sensitive parameter, it shows the largest differentiation. The variation coefficient of the velocity

No	Region	Well	Interval	Number of layers	Age	Lithology %	
1.	W. Siberia	Pokacheva—II	1705–2836	94	Cretaceous—Jurassic	shale sandstone aleurolite	52.0 40.0 6.0
2.	Kuibyshev region	Il'men'—4	502–2310	93	Carboni-ferous—Permian	limestone dolomite sandstone shale aleurolite	72.0 13.0 6.0 5.0 4.0
3.	Kuibyshev region	Il'men'—5	600–2290	70	Carboni-ferous—Permian	limestone dolomite sandstone shale aleurolite	65.0 20.0 8.0 4.0 3.0
4.	Vicinity of Krasnodar	Saratov—10	594–2666	199	Paleogene—Neogene	shale aleurolite marl sandstone limestone	45.0 41.0 6.0 5.0 3.0
5.	Vicinity of Krasnodar	Troitsk—1631	345–1515	124	Neogene	shale sand aleurolite sandstone	56.0 18.0 15.0 11.0
6.	Vicinity of Krasnodar	Podsol-nechnaya—15	2365–3-541	123	Cretaceous—Paleogene	shale limestone sandstone aleurolite	42.0 26.0 25.0 7.0
7.	Vicinity of Krasnodar	Uro-zhainoe—50	2379–2650	23	Cretaceous—Neogene	limestone shale chalk	46.0 28.0 26.0
8.	Kaspi region	Smolyan—I	4213–4678	36	Cretaceous	limestone sandstone shale	70.0 18.0 12.0
9.	Kaspi region	Russky Khutor—95	1200–2300	74	Paleogene	shale aleurolite sandstone	36.0 32.0 32.0

$\sigma_V/\overline{V}$ varies from 0.054 to 0.169, its mean value being 0.102. The parameter $\sigma_\rho/\overline{\rho}$ varies between 0.031 and 0.056, with a mean of 0.041. On the basis of the ratio of the coefficients of variation the terrigeneous* formations can be definitely distinguished from the terrigeneous—carbonate ones. In the first, the ratio of the coefficients of variation is 1.5–2.35; in the second, 2.37–4.02. Consequently, taking into account Eqs. (9)–(11), the coefficients of reflection are much more affected by the velocities than by the densities. In terrigeneous—carbonate series the densities play a very slight role in the generation of the

---

* The translation follows the author's terminology by using "terrigeneous" instead of "clastic" (Editor)

$\bar{V}$	σ_V	$\sigma_V/\bar{V}$	$\bar{\rho}$	σ_ρ	$\sigma_\rho/\bar{\rho}$	$\dfrac{\sigma_V/\sigma_\rho}{\bar{V}/\bar{\rho}}$	Interval coefficient R_z	Correlation coefficient		Coefficient	
								for intervals	mean	m	n
3642	305.8	0.084	2.53	0.142	0.056	1.50	1705–2095 2095–2480 2480–2836	− 0.040 + 0.648 + 0.601	+ 0.403	0.162	0.331
5066	568.8	0.112	2.52	0.119	0.047	2.38	502–1415 1415–2310	+ 0.956 + 0.591	+ 0.774	0.167	0.319
5512	670.7	0.122	2.64	0.115	0.044	2.77	600–1655 1655–2290	+ 0.899 + 0.981	+ 0.940	0.165	0.323
2387	149,8	0.063	2.06	0.066	0.032	1.97	594–1099 1099–1522 1522–2060 2060–2666	+ 0.539 + 0.668 + 0.570 + 0.412	+ 0.547	0.171	0.315
2073	111.6	0.054	2.09	0.067	0.032	1.69	345– 625 625–1050 1050–1515	+ 0.300 + 0.686 + 0.457	+ 0.481	0.230	0.290
4235	717.9	0.169	2.55	0.107	0.042	4.02	2365–2784 2784–3181 3181–3541	+ 0.944 + 0.776 + 0.374	+ 0.615	0.487	0.199
3523	517.9	0.147	2.47	0.113	0.046	3.20	2379–2650	+ 0.569	+ 0.569	0.365	0.233
5870	525.8	0.090	2.85	0.107	0.038	2.37	4213–4678	+ 0.843	+ 0.843	0.142	0.345
2823	205.9	0.073	2.43	0.076	0.031	2.35	1200–1850 1850–2300	+ 0.856 + 0.348	+ 0.602	0.107	0.391

reflected waves whereas in mainly terrigeneous formations they have a significant effect; as a matter of fact in some particular intervals the whole dynamics of the wave is governed by the density variations. This should be especially evident if we analyse the coefficients of correlation with depth. If in the terrigeneous—carbonate series there exists a strong positive correlation between V and ρ $(0.57 < R_z < 0.94)$, then a much weaker relationship belongs to the terrigeneous rocks $(0.40 < R_z < 0.60)$. As a general consequence of this, by Eqs. (9)–(11) the mean value of the reflection coefficients will be much higher in the

carbonate sections, implying an increased activity of the inter-bed multiples, in accordance with the available experimental evidence. From the point of view of the recovery of the petrophysical properties from the seismic data, the quantitative relationships obtained show that in essentially carbonate or ter-rigeneous—carbonate series the form of the pseudo-acoustic log can be compared without significant errors with the values of the sonic log. In terrigeneous series, however, no comparison with the PAL can be found unless both the sonic log and the GGL are available. Substantial differences could exist between the PAL and SL curves that are due to the absence of density information, rather than to the erraneous computation of the PAL.
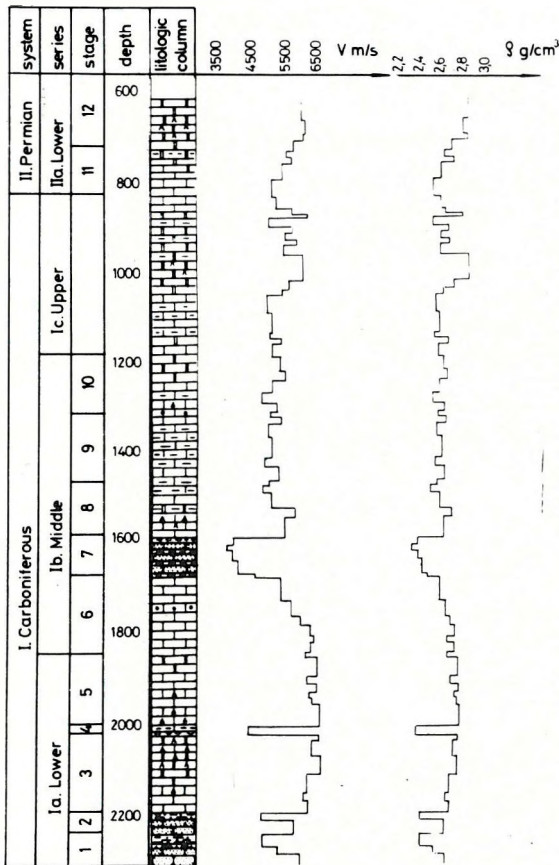

Fig. 2. Il'men'—5 Well. *In situ* values of V and ρ
Stages: 1 — Bobrovka; 2 — Tula; 3 — Oka; 4 — Tarusa; 5 — Serpukhov; 6 — Bashkirian; 7 — Vereiski; 8 — Kashira; 9 — Podol'sk; 10 — Myach-kovo; 11 — Assel; 12 — Artinsk—Sakmara

2. ábra. Il'men'—5. sz. fúrás. V és ρ *in situ* értékei
I — karbon; Ia — alsó, Ib — középső, Ic — felső; II — perm; IIa — alsó.
Emeletek: 1 — Bobrovka; 2 — Tula; 3 — Oka; 4 — Tarusza; 5 — Szerpu-hov; 6 — Baskír; 7 — Vereiszki; 8 — Kasira; 9 — Podoliai; 10 — Mjacsko-vo; 11 — Asszel; 12 — Artinszk—Szakmara

Рис. 2. Скв. Ильменевская 5. Графики пластовых значений V и ρ
I — Карбон, Ia — нижний, Iб — средний, Iц — верхний, II — Пермская, IIa — нижняя.
Ярусы: 1 — Бобровский; 2 — Тульский; 3 — Окский; 4 — Тарусский; 5 — Серпуховский; 6 — Башкирский; 7 — Верейский; 8 — Каширский; 9 — Подольский; 10 — Мячковский; 11 — Асселский; 12 — Артинский—Сакмарский

A striking example for the above argumentation will be provided if we consider the results of an analysis of the Pokacheva-II Well, West Siberia. There is an interval within the productive layer where there is a zero (or slightly positive) correlation between V and ρ. If we also take into account that the coef ficients of variation of V and ρ are anomalously low in this part of the section,

it can surely be stated that any modelling of the wave field within this layer, any PAL processing or interpretation, should be based on a joint interpretation of the SL and GGL data. Without this, no meaningful conclusions are obtainable.
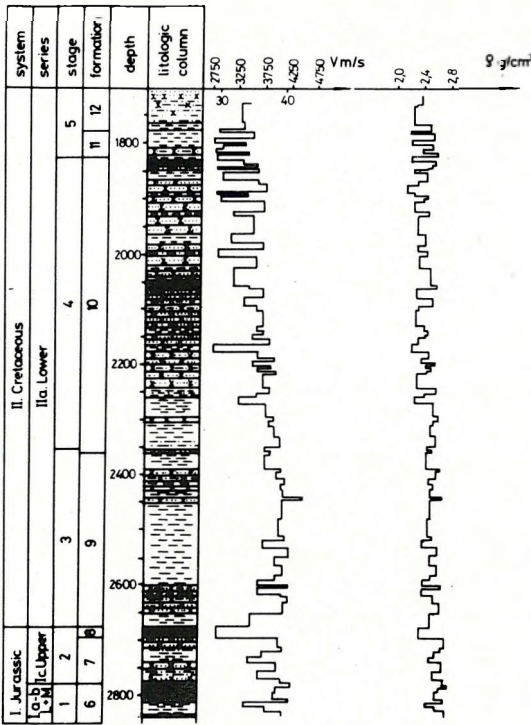

Fig. 3. Pokacheva—II Well. *In situ* values of V and ρ
Stages: 1 — Toarcian; 2 — Callovian—Volga; 3 — Berriasian—Valanginian; 4 — Hauterivian—Barremian; 5 — Aptian + Albanian + Cenomanian. Formations: 6 — Tyumen; 7 — Vasyugan, 8 — Bazhenovo; 9 — Megion; 10 — Vartovo; 11 — Alymka; 12 — Pokur

3. ábra. Pokacseva—II. sz. fúrás V és ρ *in situ* értékei
I — Jura; Ia—b — alsó + középső; Ic — felső; II — kréta; IIa — alsó. Emeletek: 1 — toarci; 2 — kallovi—volgai; 3 — berriasi—valangini; 4 — hauterivi—barrémi; 5 — apti + albai + cenomán.
Formációk: 6 — Tyumen; 7 — Vaszjugan; 8 — Bazsenovo; 9 — Megion; 10 — Vartovo; 11 — Alümka; 12 — Pokur

Рис. 3. Скв. Покачевская II. Графики пластовых значений V и ρ

I — Юрская, Ia—б — нижний + средний, Iц — верхний, II — Меловая, IIa — нижний
Ярусы: 1 — Тоарский; 2 — Келловей—Волжский; 3 — Берриас—Валанжинский; 4 — Готеривский + Барремский; 5 — Апт. + Альб. + Сеноманский.
Свиты: 6 — Тюменьская; 7 — Васюганская; 8 — Баженовская; 9 — Мегионская; 10 — Вартовская; 11 — Алымская; 12 — Покурская

Incidentally, it is by no means surprising that we have encountered such an anomalous layer in a terrigeneous section for it is well known that the two basic lithotypes of the terrigeneous formations, viz. sandstones and shales, are characterized by an inverse relation between velocity and density: on the average, the velocity is higher in sandstones than in shales [SHERIFF 1980, BULATOVA et al. 1970, DORTMAN 1976], while the shale density is generally higher [GREGORY 1977, MAXANT 1980, TUREZOVA et al. 1975]. In other words, in an idealized alternating sand/shale sequence the velocity increase during a shale/sand transition will be counteracted by a density drop; that is, the $V(z)$ and $\rho(z)$ curves will have a negative correlation.

The quantitative relationships between V and ρ are also important if one has to estimate or predict one of the parameters from the other. The mutual relationships are plotted for several wells in Fig. 4(a, b). In all cases the relationship is fairly well approximated by a formula of type (1), with the coef ficients m and n given in Table I. *Fig. 5* presents the mutual relationship for the same lithology and for all wells. The quantitative characteristics practically coincide for the sandstones and shales ($m = 0.190$ and 0.189, $n = 0.309$ and 0.312, respectively). For limestones the relationship is nearly linear, taking into account the large scatter, however, one can also use an approximation of form (1) without too large errors, and the coefficients will be close even to those for sandstones and shales.
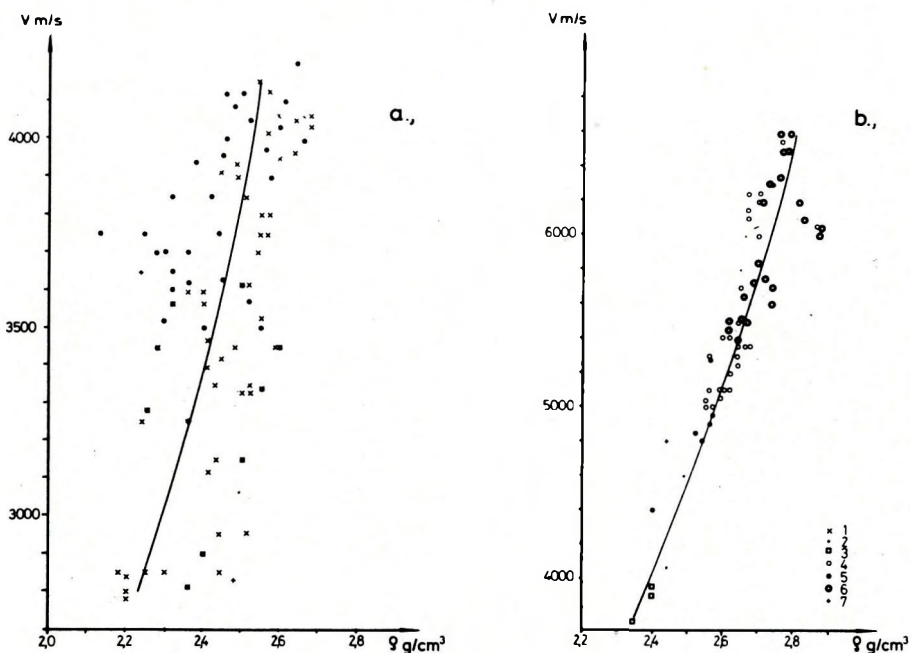

Fig. 4. Plots showing the $V = f(\rho)$ relationship
a) Pokacheva—II Well, b) Il'men'—5 Well
Conditional notations: 1 — shale; 2 — sandstone; 3 — shaly sandstone; 4 — limestone;
5 — shaly limestone; 6 — dolomite; 7 — aleurolite

4. ábra. A $V = f(\rho)$ összefüggés
a) Pokacseva—II fúrás, b) Il'men'—5 fúrás
Feltételes jelölések: 1 — pala; 2 — homokkő; 3 — palás homokkő; 4 — mészkő;
5 — palás mészkő; 6 — dolomit; 7 — aleurolit

Рис. 4. Графики зависимости $V = f(\rho)$
a) Скв. Покачевская II, b) Скв. Ильменевская 5.
Условные обозначения: 1 — глина, 2 — песчаник, 3 — песчаник глинистый,
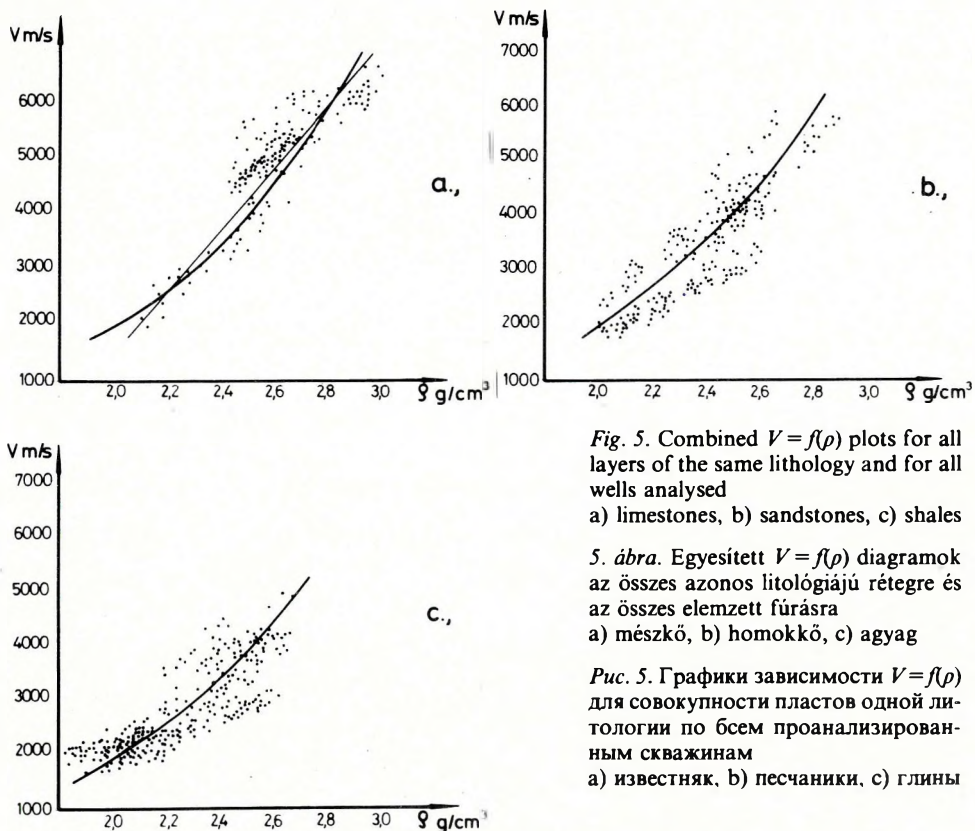4 — известняк, 5 — известняк глинистый, 6 — доломит, 7 — алевролит

Fig. 5. Combined $V = f(\rho)$ plots for all layers of the same lithology and for all wells analysed
a) limestones, b) sandstones, c) shales

5. ábra. Egyesített $V = f(\rho)$ diagramok az összes azonos litológiájú rétegre és az összes elemzett fúrásra
a) mészkő, b) homokkő, c) agyag

Рис. 5. Графики зависимости $V = f(\rho)$ для совокупности пластов одной литологии по бсем проанализированным скважинам
a) известняк, b) песчаники, c) глины

In most cases connected with the solution of the inverse problem we have to study the effect of the densities on the reflection coefficients determined from sonic logs, and on the low-frequency components of the distribution of the reflection coefficients computed from estimated interval velocities or from well velocity surveys. In these cases we have from Eq. (1):

$$K = \frac{V_{i+1}\rho_{i+1} - V_i\rho_i}{V_{i+1}\rho_{i+1} + V_i\rho_i} = \frac{V_{i+1}^{1+n} - V_i^{1+n}}{V_{i+1}^{1+n} + V_i^{1+n}} \tag{13}$$

that is, from the point of view of the computation of the reflection coefficients, only the exponent n of Eq. (1) has any effect. It has been found, however, that the value of n is quite stable for different wells and lithologies: it is around 0.304 ± 0.032 (In GARDNER et al. (1974) a similar value of $n = 0.25$ is reported on the basis of laboratory studies on core samples).

It can be stated that for terrigeneous—carbonate series, in the absence of hydrochemical sediments and coals, one can use the estimated value of n in order to predict the reflection coefficients from measured velocity data.

In those series, however, where salt, gypsum, anhydrite or coal are present, we have first of all to separate these rocks. Their density can be estimated fairly well from the lithology since their densities (as well as velocities) have only a very slight variability. According to the published data compiled in DORTMAN (1976), the following density values can be used:

salt	2.16 g/cm³
gypsum	2.37 g/cm³
anhydrite	2.96 g/cm³
coal	1.40 g/cm³

5. Conclusions

It has been shown that the dispersion of the values of the reflection coefficients is determined by the coefficients of variation of the velocities and densities occurring in the section, and by the degree of correlation between these parameters.

Directly measured longitudinal wave velocities and density values were presented, obtained in wells of some of the most important oil-producing regions. It has been shown that in series containing a large fraction of carbonate rocks the variation coefficient of the velocity is significantly larger than that of the density, and there is a clear-cut positive correlation between V and ρ if they are considered as functions of depth. If the geoseismic modelling is carried out under these conditions, the proper scaling of the pseudo-acoustic transformation and the comparison of the pseudo-acoustic log can be carried out on the basis of the sonic log alone, by estimating the density values from the velocities. In terrigeneous sediments the coefficients of variation of the velocities and densities are very close, and the correlation between V and ρ is significantly less. In such cases direct velocity and density measurements should be utilized to analyse the seismic data.

In some productive layers of West Siberia there appears an interval between the Alymka Formation and the lower third of the Vartovo Formation where the correlation between velocity and density abruptly deteriorates, up to an interval where even negative correlations appear. In such cases of course, no meaningful modelling or computation of the pseudo-acoustic logs can be carried out on the basis of the sonic log alone.

We have analysed the mutual connection between velocity and density for different wells and various lithotypes of rocks. It has been shown that for practically all cases the connection can be approximated fairly well by a law of form (1). The quantitative values of the coefficients to be used in the prediction of the densities of the rocks from the velocities have also been determined.

REFERENCES

AGARD, J. 1961: Analyse statistique et probabilistique des sismogrammes. Rev. Inst. Franc. du Petrole, **16**, 3, pp. 1–48; 4, pp. 49–85

AROV, B. I. 1981: Physical properties of rocks and some questions concerning the modelling of geophysical fields in the prospecting of oil (in Russian). In: "Methodical questions and some results of oil exploration in the Pripyat Depression", Nauka i Tekhnika, Minsk, pp. 82–94

BEREZKIN, V. M. 1963: On the connection between the density of rocks and the velocity of elastic waves propagating in them (in Russian). Razv. i Promysl. Geofizika, **49**, pp. 86–88

BOIS, P., HEMON, CH. 1963: Étude statistique de la contribution des multiples aux sismogrammes synthetiques et reels. Geoph. Prospecting, **11**, 3, pp. 313–349

BULATOVA, ZH. M., VOLKOVA, E. A., DUBROV, E. F. 1970: Sonic Logging (in Russian). Nedra, Leningrad, 264 p.

DORTMAN, N. B. (Ed.) 1976: Physical properties of rocks and useful minerals (in Russian). Nedra, Moscow, 527 p.

GARDNER, G. H. F., GARDNER, L. W., GREGORY, A. R. 1974: Formation velocity and density — The diagnostic basics for stratigraphic traps. Geophysics, **39,** 6, pp. 770–780

GOGONENKOV, G. N. 1972: Computation and applications of synthetic seismograms (in Russian). Nedra, Moscow, 167 p.

GOGONENKOV, G. N., ASRIYANTS, L. YA. 1969: Statistical characteristics of the distribution of reflection coefficients of elastic waves in real media (in Russian). Izv. AN SSSR Ser. Fiz. Zemli, **12,** pp. 57–61

GOGONENKOV, G. N., ZAKHAROV, E. T., EL'MANOVICH, S. S. 1980: The prediction of a detailed velocity section from seismic data (in Russian). Prikl. Geofizika, **97,** pp. 58–72

GREGORY, A. R. 1977: Aspects of rock physics from laboratory and log data that are important to seismic interpretation. In: "Seismic Stratigraphy — Applications to Hydrocarbon Exploration". Am. Ass. Petr. Geol. Tulsa, pp. 15–47

GULIN, YU. A. 1975: The gamma–gamma method for the prospecting of oil wells (in Russian). Nedra, Moscow, 154 p.

ISHII, J. et al. 1975: A study on the relationship between seismic reflection data and logging data, velocity and density. J. of the Japanese Ass. Petr. Technologists, **40,** 3, pp. 17–29

LAVERGNE, M., WILLM, C. 1977: Inversion of seismograms and pseudo velocity logs. Geoph. Prospecting, **25,** 2, pp. 231–250

MAXANT, J. 1980: Variation of density with rock type, depth and formation in the Western Canada basin from density logs. Geophysics, **45,** 6, pp. 1061–1076

MIKHAILOV, I. N. 1965: Correlation between the density and elastic wave propagation velocity in sedimentary rocks (in Russian). Prikl. Geofizika, **45,** pp. 119–130

SHERIFF, R. I. 1980: The use of seismic information for the prediction of rock properties. In: Results of Oil Geology (Russian translation). Nedra, Moscow, pp. 245–276

TUEZOVA, N. A., DOROGONITSKAYA, L. M., DEMINA, R. G., BRYUZGINA, N. N. 1975: Physical properties of the rocks of the W. Siberian oil-gas province (in Russian). Nedra, Moscow, 184 p.

VELZEBOER, C. V. 1981: The theoretical seismic reflection response of sedimentary sequences. Geophysics, **46,** 6, pp. 843–853

G. N. GOGONENKOV, JU. V. KRASZAVIN

AZ ÜLEDÉKES KŐZETEK LONGITUDINÁLIS HULLÁM-SEBESSÉGE ÉS SŰRŰSÉGE KÖZTI ÖSSZEFÜGGÉSEK VIZSGÁLATA

Annak érdekében, hogy a szeizmikus csatornák pszeudo-akusztikus transzformációjával nyert görbék kiértékelésének kritériumait meg tudjuk határozni, elemezzük az Ural—Volga vidékén, a Kaukázus előterében és Nyugat-Szibéria területén lévő kutakban mért szónikus és gamma—gamma karotázs eredményeket. Kiszámítjuk a sebesség—sűrűség változások együtthatóit és elemezzük az egyes paraméterek közti korrelációt.

Megmutatjuk, hogy a sebesség és sűrűség közti korreláció mértéke nagyban függ a formáció litológiájától, és erre a szeizmikus csatornák inverziója során figyelemmel kell lenni.

Г. Н. ГОГОНЕНКОВ, Ю. В. КРАСАВИН

СООТНОШЕНИЕ СКОРОСТЕЙ РАСПРОСТРАНЕНИЯ ПРОДОЛЬНЫХ ВОЛН И ОБЪЕМНОЙ ПЛОТНОСТИ В ОСАДОЧНЫХ РАЗРЕЗАХ

С целью разработки критериев интерпретации кривых псевдоакустического преобразования сейсмических трасс проанализированы результаты измерения акустическим и гамма—гамма каротажами в скважинах Урало—Поволжья, Предкавказья и Западной Сибири. Рассчитаны коэффициенты вариации скоростей и плотностей, проанализированы их корреляционные зависимости.

Показано, что степень корреляции между скоростью и плотностью сильно зависит от литологии разреза и это должно учитываться при инверсии сейсмических записей.

CORRELATION OF ATTENUATION OF ELASTIC WAVES WITH OTHER PETROPHYSICAL AND LITHOLOGICAL PROPERTIES

László GOMBÁR*

The paper summarizes the basic mechanisms of seismic wave absorption and the effect of the different petrophysical and geological factors on the coefficient of absorption. Laboratory experiments were performed in order to study the connection between the logarithmic decrement and the longitudinal propagation velocity in different types of rocks. For shales and sands an inverse relationship has been found between the attenuation parameter and the velocity, for fresh andesites the relationship is of the opposite direction. The main task was to check a hypothesis of SAVIT and MATEKER [1971], according to which the sedimentary rocks (shale, sand, limestone) can be distinguished on the $a—V$ diagram. According to the analysis of the laboratory data, this lithologic discrimination can be carried out only if the attenuation and velocity values are reduced to the same reference depth on the basis of known attenuation—depth and velocity—depth dependences.

d: elastic waves, attenuation, absorption, physical properties, laboratory studies

1. Introduction

In up-to-date seismic prospecting, new possibilities are given by digital data-acquisition techniques and true-amplitude-preserving processing for determining seismic parameters that are directly related to the lithology of the layers. From the point of view of elastic wave propagation the most important parameters are the propagation velocity and wave attenuation. Both parameters can be determined by seismic methods and their joint study enables a more reliable estimation of the lithology.

The attenuation of the amplitudes of elastic waves propagating in rocks is due to several effects. One of the most significant is spherical divergence that can exceed by several times the effect of absorption. Before determining the absorption coefficient one has to correct for the disturbing effects of the other of attenuation factors; the inaccuracy of these corrections, however, makes the correct determination of the absorption very difficult. SAVIT and MATEKER (1971) proposed that the most common sedimentary rocks could be distinguished on the basis of their absorption coefficient and velocity as indicated in *Fig. 1.*

The paper first summarizes the most commonly applied parameters describing the dissipation of energy during wave propagation. Basic absorption mechanisms and the petrophysical and geological factors affecting the absorption are reviewed, together with the laboratory methods for determining the absorption parameters. Next, relations are presented, obtained in laboratory measurements on different kinds of rocks, connecting the logarithmic decrement with ultrasonic velocity, and with the depth of the rock.

* Eötvös Loránd Geophysical Institute of Hungary;
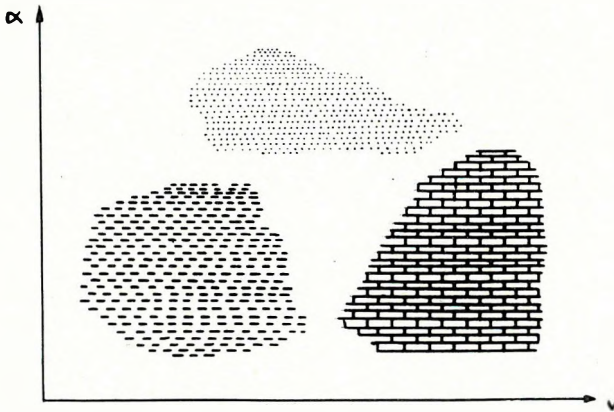 POB 35. Budapest, H—1440

Fig. 1. Lithologic distinction of sedimentary rocks (sand, shale, limestone) on the basis of their attenuation and velocity (after SAVIT and MATEKER 1971)

1. ábra. Az üledékes kőzetek (homok, agyag, mészkő) litológiai osztályozása a csillapodás—sebesség alapján (SAVIT és MATEKER 1971 nyomán)

Рис. 1. Литологическая классификация осадочных пород (песка, глины, известняка) по затуханию и скорости (по САВИТУ и МАТЕКЕРУ, 1971)

2. Parameters describing the absorption of elastic waves

For planar elastic waves propagating in not totally elastic rocks the wave amplitude (A) decreases with the distance (R) travelled according to the law $A(R) = A_0 \exp[-a(f)R]$. The attenuation of the waves, i.e. the energy-dissipating property of the rock, is usually characterized by one of the following interrelated quantities:

a — absorption coefficient
δ — logarithmic decrement
Q — quality factor.

The absorption coefficient (a) describes the relative amplitude decrease at unit distance:

$$a(f) = \frac{1}{R_2 - R_1} \ln \frac{A(R_1, f)}{A(R_2, f)} \qquad (1)$$

and

The logarithmic decrement (δ) expresses the dissipation of energy along a path corresponding to the wavelength. It is related to the coefficient of absorption as

$$\delta = \frac{V(f)a(f)}{f} \qquad (2)$$

The quality factor Q is defined by the expression

$$\frac{\Delta E}{E} = \frac{2\pi}{Q} \qquad (3)$$

where E is the total energy, ΔE the fraction of energy dissipated during a period.

An equivalent definition of Q is provided by

$$Q = \frac{\pi f}{a(f)V(f)} \tag{4}$$

As seen from Eqs. (2) and (4), the propagation velocity of elastic waves is a function of frequency, $V = V(f)$. In a narrow frequency band, however, this frequency dependence does not exceed a few per cent, so that the velocity-dispersion can be neglected in practical applications and the $V(f) \approx V_P = $ const. approximation can be used. Field investigations and laboratory studies carried out on different kinds of rocks have shown that, in the case of dry rocks, the Q factor characterizing the interior friction only slightly depends on frequency and can be considered as approximately constant in the seismic and sonic frequency range [TOKSÖZ et al. 1979]. This also implies that, if the velocity dispersion can also be neglected, the absorption coefficient is a linear function of frequency:

$$a(f) = \frac{\pi}{QV(f)} \cdot f \approx k \cdot f \tag{5}$$

ATTEWELL and RAMANA [1966], studying a large number of published data, and using the method of least mean squares found a frequency dependence of the form

$$a(f) = 1.012 \cdot 10^{-5} f^{0.911} \text{ dB/m} \tag{6}$$

for the frequency range $1-10^8$ Hz.

3. Mechanisms of absorption

The basic cause of the linear frequency dependence of the absorption coefficient of elastic waves in rocks has still not been unambiguously clarified, very possibly it is a joint effect of several physical phenomena. The physical mechanism of absorption has been treated in a great number of papers, the mechanisms proposed thus far can be grouped as follows [cf. MAVKO et al. 1979]:

— loss in connection with the viscous fluid filling the pores,
— loss derived from the properties of the solid rock matrix,
— thermoelastic effect,
— scattering (and other) losses.

According to laboratory measurements the fluid content of the rocks plays a significant part in the absorption mechanisms. Even a few per cent fluid content abruptly increases the energy dissipation as compared with a dry rock, since the wetting of the grain surfaces decreases the intergranular cohesion

[TITTMAN et al. 1972]. For greater fluid saturations the relative displacements between the fluid and solid phases due to the periodic elastic stresses, as well as the viscous stresses induced in the fluid, also increase the absorption [JOHNSTON et al. 1979]. According to WINKLER and NUR [1982] the quality factors Q Q_S, characterizing longitudinal and shear waves, respectively, are more sensitive to changes of fluid content than the corresponding velocities and, consequently, are better indicators for detecting oil- or gas-bearing layers.

As for the solid rock matrix, it can be stated that the inherent inelasticity of the constituent grains and crystals can be neglected compared with the frictional losses along grain boundaries and the surfaces of microcracks [TOKSÖZ et al. 1979]. The quality factor Q is of order of 10^3-10^5 in monocrystals, while in a rock consisting of the same crystals it is only of the order of 10^1-10^2. From among the further mechanisms of absorption the scattering losses are considered as the most significant. The elastic waves are scattered at the surfaces (edges, vertices) of the constituents of a polycrystalline or granular rock, their amplitude decreases. This effect might become significant if the wavelength approaches the characteristic size of the inhomogeneities [BRADLEY and FORT, 1966].

Generally, the amount of dissipation and the frequency dependence of the absorption coefficient are determined by a superposition of the above effects. The relative importance of these phenomena, however, is greatly influenced by the characteristic lithological, petrophysical and geological parameters of the rock. With porous rocks the absorption coefficient and the longitudinal propagation velocity are influenced [according to MILITZER and SCHÖN, 1972] by

— rock texture,
— cementation and cohesion of the grains,
— elasticity and size distribution of the grains,
— porosity and fluid saturation,
— properties of the pore content,
— pressure, depth, geologic age, temperature,
— the applied frequency.

The absorption mechanisms and the dependence of absorption on the rock-physical parameters have thus far been mainly studied under laboratory conditions, on core samples. Since these measurements are carried out in the sonic and ultrasonic frequency range, their results cannot immediately be extrapolated to the relatively narrow 10–250 Hz band of the *in situ* frequency measurements. The results of the measurements on core samples can, however, be brought into a closer correspondence with the seismic elastic and dissipation parameters by means of sonic logs and VSP surveys.

4. Laboratory measurement of the absorption parameters

There exist several published methods for the laboratory determination of the absorption parameters. It is a general problem in these kinds of measurement that the energy losses arising at the sample—instrument coupling, or depending on specimen geometry, have to be taken into proper account. The following are the most widely used measurement techniques:

1. The method based on the phase difference between a slowly changing periodic stress and the induced periodic deformation [BORN 1941].
2. The method determining the amplitude decrease of a harmonic, monochromatic signal [TOKSÖZ et al. 1979].
3. The method determining the amplitude decrease of an impulse, multiply reflected at the parallel facets of the rock specimen [TRUELL et al. 1969].
4. The resonance method [BORN 1941, SCHREIBER et al. 1973].

The resonance method requires the simplest instrumentation. A cylindrical rock sample, secured at its centre, is periodically vibrated at one end, i.e. the bar exercises a forced vibration. The dilatational vibration amplitude of the bar becomes maximum if some integer multiple of the half wavelength of the induced vibration agrees with the length of the rod: $n\frac{\lambda}{2} = L$. The dissipation factor Q can be determined in terms of the resonance frequency f_r and the resonance band-width Δf as

$$Q = \frac{f_r}{\Delta f} \tag{7}$$

where Δf is the difference of the two frequencies around f_r where the amplitude falls to $1/\sqrt{2}$ times its maximum value. It can be shown that this definition is equivalent with Eq. (3) [see TRUELL et al. 1969]. The method presupposes that only longitudinal displacements occur in the sample, i.e. the transverse vibration modes can be neglected. Equation (7) is not exact unless the length of the specimen is much greater than its diameter. If this is not satisfied, the measured resonance frequencies should be corrected according to the Rayleigh formula [SCHREIBER et al. 1973].

We have studied the connection between the absorption parameter and the longitudinal propagation velocity in different types of rocks by means of laboratory measurements. Core samples were taken from two Hungarian locations: the Oligocene shaly and sandy rocks from a bore-hole in Mány, the Miocene andesite samples from a borehole around Nagymaros.

The absorption parameter was determined by the resonance method, the longitudinal velocity by a direct measurement of the transit time of the elastic impulse.

5. Connection of absorption parameter with longitudinal velocity and with depth

From the measured data it seemed most convenient to search for a relationship between the longitudinal velocity and the logarithmic decrement and to check the fulfilment of the SAVIT–MATEKER [1971] hypothesis between these quantities. In recent literature there are only a few reports on similar experiments. C. RAMACHANDRAN and M. RAMACHANDRAN [1981] carried out absorption and velocity measurements on Carboniferous, Permian and Triassic sandstones and shales and found a relationship of the form

$$a = A - BV_P \qquad (8)$$

From the Russian literature, a similar relationship is reported by IVAKIN et al. [1978] for sandstones and marls, on the basis of sonic logs.

It is more convenient to use Q or δ instead of a because of the frequency- and velocity-dependence of the latter. For our laboratory data the corresponding pairs of logarithmic decrement and longitudinal velocity values were better fitted by the expression

$$\delta = A V_P^n \qquad (n < 0) \qquad (9)$$

than a linear relationship. For example, for shaly rocks there corresponded a correlation coefficient $R = -0.69$ to the linear fit

$$\delta = 0.308 - 0.072 \ V_P \qquad (10)$$

while the relationship

$$\delta = 0.243 \ V_P^{-0.649} \qquad (11)$$

was satisfied by $R = -0.79$. For sands the correlation coefficient corresponding to Eq. (9) is greater by only 0.04 than that corresponding to Eq. (8); for andesites the difference is only 0.02, i.e., by proceeding towards more compacted rocks relation (9) gradually goes over to the linear relation (8):

	A	n	R
shales	0.245	-0.649	-0.79
sands	0.226	-0.462	-0.52
andesites	0.182	-0.350	-0.42
fresh andesites	0.080	0.236	$+0.30$

The determination of the values of A, n and R was made by the least mean squares method (V_P is given in km/s). The absolute values of A and n gradually decrease from the shales towards the andesites. With shales and sands there is
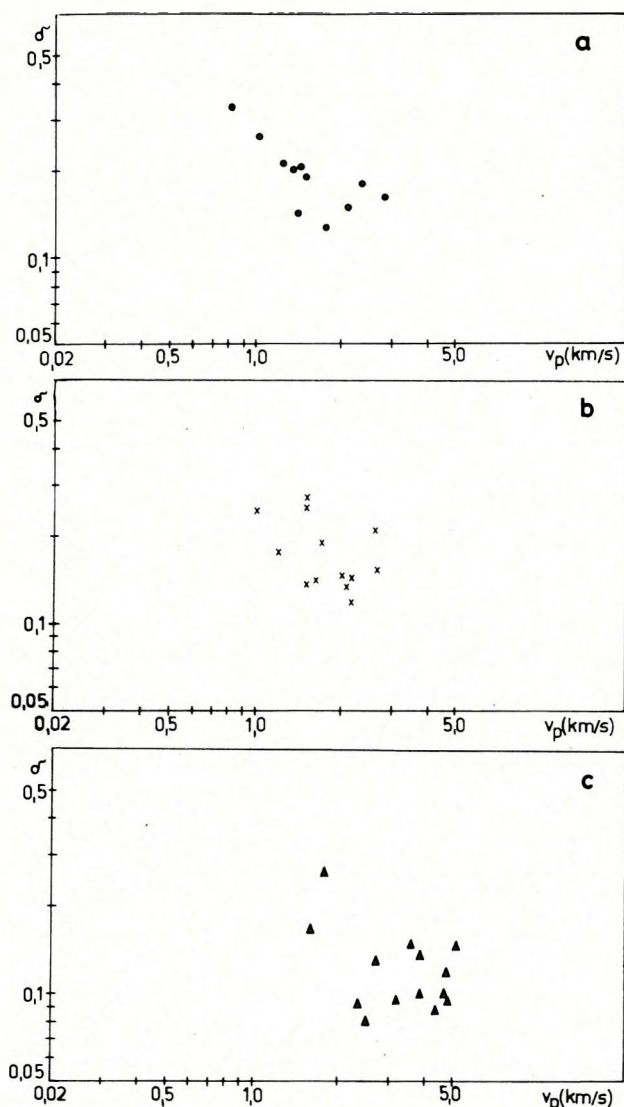
Fig. 2. Connection between logarithmic decrement and longitudinal velocity for shales and shaly marls (a), sands (b) and andesites (c)

2. ábra. A logaritmikus dekrementum—sebesség kapcsolata agyagok (a), homokok (b), andezitek (c) esetében

Рис. 2. Связь логарифмического декремента со скоростью для глин и глинистых мергелей (a), песков (b) и андезитов (c)

an unambiguous inverse relationship between δ and V_P *(Figs. 2a, 2b)*. For the andesites, however, this relationship is not that clearcut—by considering the fresh andesites we can even observe an opposite tendency (*n* becomes positive, see *Fig. 2c*). PAVLENKIN [1967] presented a similar "opposite" relationship between the velocity and logarithmic decrement values measured in granites. MARLE's [1980] anisotropy measurements also seem to suggest that for intrusive rocks the absorption parameter increases with velocity. So, on the basis of the very few measured or published data, it can be supposed that for certain types of magmatic rocks there exists an anomalous relationship between the velocity and the absorption parameter.

Fig. 3 shows the absorption coefficients belonging to the resonance frequencies. For the individual rock types the linear law $a = kf$ is fairly well satisfied. According to the slope of the lines we can distinguish three domains on the diagrams. Fresh andesites are situated between the straight lines of slope $k = 2 - 5 \cdot 10^{-5}$. For the more compacted sandstones and shaly marls the value of k varies from $6 \cdot 10^{-5}$ to $8 \cdot 10^{-5}$. The loosest sands, shales, decomposed andesites cluster around the straight line of slope $13 \cdot 10^{-5}$ or on the left side of it.
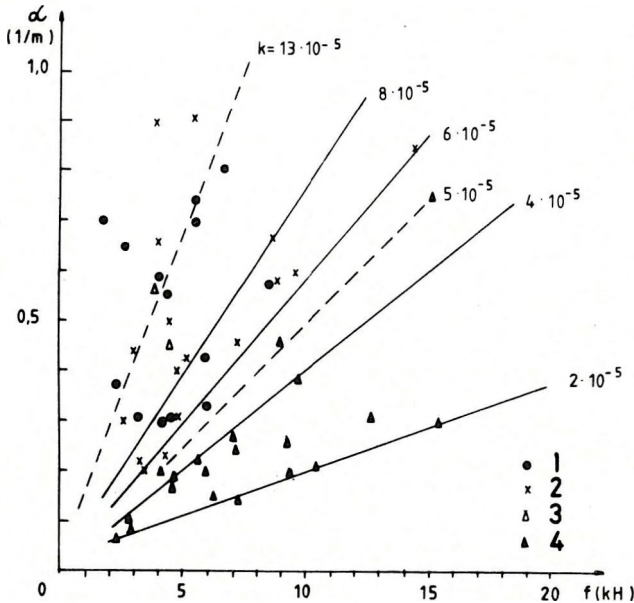

Fig. 3. Frequency-dependence of the absorption coefficient for the rocks studied, on the basis of the resonance frequencies
1 — shale and shaly marl; 2 — sand; 3 — decomposed andesite; 4 — fresh andesite

3. ábra. Az abszorpciós együttható frekvencia függése a vizsgált kőzetekre vonatkozóan, a rezonanciafrekvenciák alapján
1 — agyag és agyagmárga; 2 — homok; 3 — bontott andezit; 4 — üde andezit

Рис. 3. Зависимость коэффициента поглощения от частоты для изучаемой породы по резонансным частотам.
1 — глина и глинистая мергель, 2 — песок, 3 — выветрившийся андезит, 4 — свежий андезит

On the $\delta - V_P$ diagram of *Fig. 4* the fresh andesites are fairly well separated from the sedimentary rocks, the distinction between the shales and sands however cannot be judged as clearly as would have been anticipated on the basis of the SAVIT–MATEKER [1971] hypothesis. A possible cause of this discrepancy could lie in the transitional character of the lithology of the rocks studied (sandy shale, shaly sand, etc.). Also, for the younger, only partially consolidated sedimentary rocks both the absorption parameter and the propagation velocity could considerably depend on depth. The basic cause of this depth-dependence is the decreasing porosity of the rocks with depth due to compaction.

Fig. 5 shows the logarithmic decrement of the rock samples as a function of depth, for the 200–400 m depth range. For this depth range δ decreases with depth approximately exponentially, in accordance with the findings of MILITZER and SCHÖN [1972] and GARDNER et al. [1964] (the velocity does not show a systematic variation along this depth range).
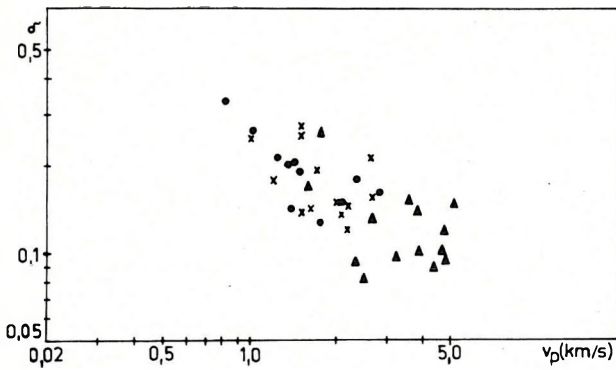
Fig. 4. Lithologic classification of rocks on the basis of the logarithmic decrement and the longitudinal velocity. Key as in Fig. 3.

4. ábra. A kőzetek litológiai osztályozása a logaritmikus dekrementum—longitudinális sebesség alapján

Рис. 4. Литологическая классификация горных пород по логарифмическому декременту и продольной скорости. Объяснение условных обозначений приведено на рис. 3.
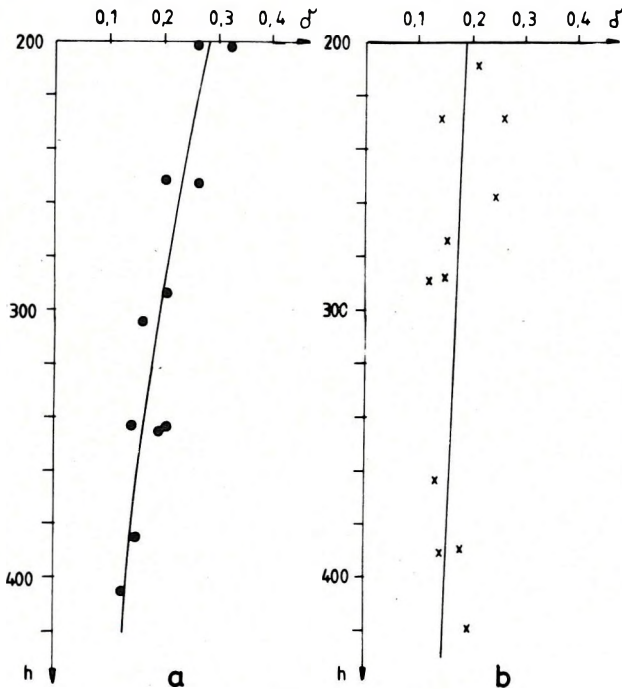

Fig. 5. Connection between logarithmic decrement and depth, for shales (a) and sands (b)

5. ábra. A logaritmikus dekrementum—mélység kapcsolat, agyagok (a) és homokok (b) esetében

Рис. 5. Связь между логарифмическим декрементом и глубиной для глин (a) и песков (b)

Using a least mean squares fit, we obtain the relationship

$$\delta = 0.581 \exp\left[-3.63 \cdot 10^{-3}\, h\right] \tag{12}$$

$$R = -0.88$$

for shales, and

$$\delta = 0.235 \exp [-1.09 \cdot 10^{-3} \text{ h}] \tag{13}$$

$$R = -0.33$$

for sandstones. The absorption parameter of shaly rocks decreases more rapidly and more systematically with depth; for sandstones we observe a large capricious fluctuation superimposed on the decreasing trend. This might be due to the fact that the compaction of porous permeable sands is governed by the difference of the lithostatic pressure and the pressure of the pore fluid, i.e. by the differential pressure, while the state of compaction of the shales corresponds to the lithostatic pressure. Consequently, for sandstone layers one can predict the changes of the pore fluid or of its pressure on the basis of the deviations of the absorption parameters from the general trend.

The $\delta(h)$ function can be used to reduce the absorption parameters of rocks from different depths to a common reference depth. For our study site this reduction can be carried out by the formulae

$$\delta(H) = \delta(h) \exp [-3.63 \cdot 10^{-3} (H-h)] \tag{14}$$

for shales, and

$$\delta (H) = \delta(h) \exp [-1.09 \cdot 10^{-3} (H-h)] \tag{15}$$

for sands, where H is the reference depth. *Fig. 6* shows the δ values, reduced to the depth $H = 500$ m by means of Eqs. (14) and (15), as a function of V_P. The values reduced to a common depth are already in a much closer connection with the lithologic properties of the layers and the sands and shales can be separated with greater certainty on the attenuation—velocity diagram, in conformity with the SAVIT–MATEKER hypothesis.
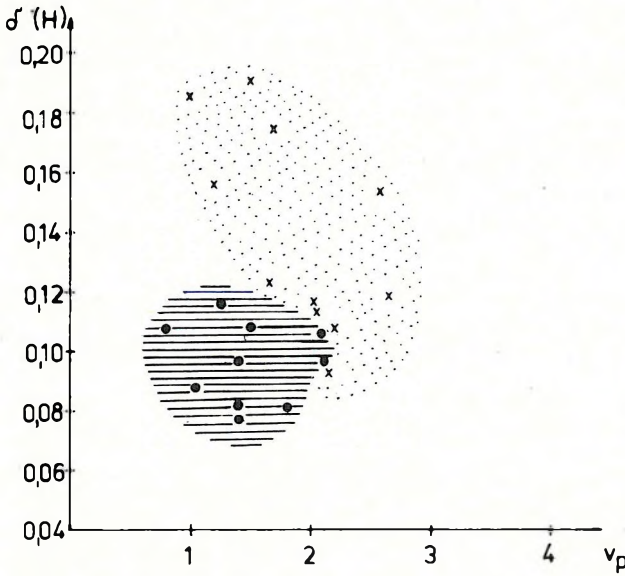
Fig. 6. Distinction between shales (shaly marls) and sands on the basis of the logarithmic decrement and the velocity values, reduced to the same reference depth ($H = 500$ m)

6. ábra. Az agyagok és homokok osztályozása az azonos mélységre ($H = 500$ m) átszámított logaritmikus dekrementum és sebesség alapján

Рис. 6. Классификация глин, глинистых мергелей и песков по приведенным к одинаковой глубине ($H = 500$ м) логарифмическому декременту и скорости.

REFERENCES

ATTEWELL, P. B., RAMANA, Y. V. 1966: Wave attenuation and internal friction as functions of frequency in rocks. Geophysics **31**, 6, pp. 1049–1056

BORN, W. T. 1941: The attenuation constant of earth materials. Geophysics, **6**, 2. pp. 132–148

BRADLEY, J. J., FORT, A. N. Jr. 1966: Internal Friction in Rocks (In: S. P. CLARK, Jr. Ed.: Handbook of physical constants.) Geol. Soc. Am. Memoir 97

GARDNER, G. H. F., WYLLIE, M. R. J., DROSCHAK, P. M. 1964: Effects of pressure and fluid saturation on the attenuation of elastic waves in sands. J.'Petr. Techn. **16**, 2, pp. 189–198

IVAKIN, B. N., KARUS, E. V., KUZNETSOV, O. L. 1978: Sonic Logging (in Russian). Moscow, Nedra

JOHNSTON, D. H., TOKSÖZ, M. N., TIMUR, A. 1979: Attenuation of seismic waves in dry and saturated rocks: II. Mechanisms. Geophysics, **44**, 4, pp. 691–711

MARLE, Ch. 1980: Some problems of anisotropic, especially elastic behaviour of rocks. Proceedings of 25th. Internat. Geophysical Symposium, Székesfehérvár, Hungary, pp. 508–516

MAVKO, G., KJARTANSSON, E., WINKLER, K. 1979: Seismic wave attenuation in rocks. Rev. of Geoph. and Space Physics **17**, 6, pp. 1155–1164

MILITZER, M., SCHÖN, J. 1972: Some theoretical and experimental results for the determination of characteristic properties of naturally bedded rocks on the basis of seismic measurements. 24th Int. Geol. Congr. Section 9 (Montreal, Canada) pp. 158–164

PAVLENKIN, A. D. 1967: Connection of the absorption decrement with the lithologic properties of the rocks and with the elastic propagation velocity (in Russian). Razv. Geof. **22**, pp. 38–44

RAMACHANDRAN, C., RAMACHANDRAN NAIR, M. 1981: Elastic properties of Lower Gondwana rocks of Eastern India. Geoexploration, **19**, 1, pp. 15–32

SAVIT, C. H., MATEKER, E. J. Jr. 1971: From "where?" to "what?" 8th World Petroleum Congr. Moscow

SCHREIBER, B., ANDERSON, O. L., SOGA, N. 1973: Elastic constants and their measurements. McGraw–Hill, Inc. New York

Tittman et al. 1972: Elastic velocity and Q measurements on Apollo 12, 14 and 15 rocks. Proc. 3rd Lunar Sci. Conf. pp. 2565–2575

Toksöz, N., Johnston, D. H., Timur, A. 1979: Attenuation of seismic waves in dry and saturated rocks: I. Laboratory measurements. Geophysics, **44**, 4, pp. 681–691

Truell, R., Elbaum, Ch., Chick, B. B. 1969: Ultrasonic methods in solid state physics. Academic Press, New York–London

Winkler, K. W., Nur, A. 1982: Seismic attenuation: Effects of pore fluids and frictional sliding. Geophysics, **47**, 1, pp. 1–15

GOMBÁR LÁSZLÓ

RUGALMAS HULLÁMOK ELNYELŐDÉSÉNEK KAPCSOLATA A KŐZETFIZIKAI ÉS LITOLÓGIAI TULAJDONSÁGOKKAL

A dolgozat összefoglalja az alapvető abszorpciós mechanizmusokat, valamint a kőzetfizikai és geológiai tényezők hatását az elnyelődésre.

Különböző kőzetekre vonatkozóan megvizsgálja a laboratóriumi mérések során kapott logaritmikus dekrementum és longitudinális sebesség kapcsolatát. Agyagok és homokok esetében az elnyelődési paraméter és a sebesség között inverz kapcsolat van, míg az üde andezitekre ez a kapcsolat ellenkező irányú. A dolgozat vizsgálja a Savit és Mateker (1971) hipotézis teljesülését, amely szerint az $a-V$ síkon az üledékes kőzetek (agyag, homok, mészkő) elkülöníthetők egymástól.

A mérési eredmények elemzése alapján megállapítható, hogy a litológiai osztályozásra csak akkor van lehetőség, ha a csillapodás és a sebesség mélységtől való függésének ismeretében egy közös szintre redukáljuk a csillapodás- és sebességértékeket.

Л. ГОМБАР

СВЯЗЬ ПОГЛОЩЕНИЯ УПРУГИХ ВОЛН С ПЕТРОФИЗИЧЕСКИМИ И ЛИТОЛОГОЧЕСКИМИ СВОЙСТВАМИ

В работе подытоживаются основные механизмы поглощения, а также влияние петрофизических и геологических факторов на поглощения.

Были проведены лабораторные измерения для изучения связи логарифмического декремента с продольной скоростью на разных породах. Для глин и песков существует обратная связь между параметром поглощения и скоростью, а для свежих андезитов такая связь состоит в противном направлении. В работе рассматривается выполнения гипотеза Савита и Матекера (1971), по которому имеется возможность разделить осадочные породы (глины, пески и известняки) по плоскости $a-V$.

По анализу результатов измерения можно отметить, что провести литологическую классификацию можно только в случае, когда на основе знания зависимости затухания и скорости от глубины значения затухания и скорости приводятся к общему уровню.

DEVELOPMENT OF INTERPRETATION METHODS
OF PSEUDO-ACOUSTIC SECTIONS ON THE BASIS
OF GEOSEISMIC MODELLING

G. N. GOGONENKOV*, N. D. PAVLOV*, V. D. LEVCHENKO*,
B. I. AGAFONOV*

The paper presents geoseismic modelling studies carried out on a geologically typcial site of the Volga—Uralian oil-gas province. Computed synthetic time sections are retransformed into acoustic impedance sections in order to study the possibilities of pseudo-acoustic logs in investigations of the fine structure and material properties of productive formations. By analysing the results and comparing them with the original input models general conclusions are drawn and requirements are formulated concerning the proper interpretation of the pseudo-acoustic sections.

d: synthetic seismograms, oil and gas fields, seislog, models, reefs

1. Introduction

The most promising new ways of increasing the efficiency of the seismic method are connected with the solution of the inverse dynamic problem, i.e. with the estimation of the detailed distribution of the elastic properties on the basis of the seismic wave field. To date, the solution to this problem has been realized in a method consisting in the inversion of the seismic traces, termed the *pseudo-acoustic transformation* or *pseudo-acoustic log* in the Russian literature [GOGONENKOV et al. 1980, GOGONENKOV–PETERSEN 1982], and "SEISLOG", "VELOG", etc. in Western technical papers [BOIS 1978, LINDSETH 1979, STREET 1978, GARDNER 1974].

Due to the fact that in this methodology the solution of the inverse dynamic problem results in an effective seismic model that does not contain the whole spectral range of the distribution of the elastic properties but only a limited part of it bounded from above by some cut-off frequency, the practical interpretation of the pseudo-acoustic sections involves certain difficulties (GOGONEN-KOV–ANTIPIN 1970). These difficulties become even more serious if in the low-frequency part of the spectrum there is also missing information on some of the spectral components. Such cases are encountered if we somehow cannot get information on the formation velocity model of the medium, or if the velocity model only describes the very low-frequency variations so that there is a gap between the frequency band of the layer model and the frequencies of the seismic trace where we have no information on the amplitude- and phase characteristics of the respective spectral components.

* Central Geophysical Expedition of the Oil Ministry, 123298 Moscow, ul. Norodnogo Opolcheniya 40, korp. 3, USSR

In order to study the distortions in the distribution of the elastic properties due to these effects, and to develop a proper methodology for the interpretation of the pseudo-acoustic sections, we have carried out model studies for typical geological situations. Study sites were selected from the seismically explored territories of the Ural—Volga region, W. Siberia and the Caucasian Fore-deeps.

The main results of this model study—besides increasing our under-standing of the proper interpretation of the pseudo-acoustic logs—will de-monstrate that there is a real possibility for the detailed delineation of the productive intervals; also, we will be able to state the requirements concerning the bandwidth of the seismic records that are necessary for solving a given geological problem.

In the present paper only a selected model study will be dealt with, in connection with a typical geological structure from the Volga—Uralian oil and gas province.

2. Method of modelling

The structures to be modelled were selected on the basis of the following criteria: typicality of the geological situation, CH-prospects, sufficiently well known with regard both to the geometry of the layers and to the elastic and density properties. As a rule, such structures were selected where a sufficient amount of geophysical well log data was available, including sonic and density logs. The model profiles are perpendicular to the srike of the main geological objects, and go through the boreholes. Using the available well-log data and the seismic sections the individual layers were correlated and a detailed geological model was constructed. The thickness of the layers varied between 5 and 30 m. Next, on the basis of the available sonic and gamma—gamma logs, the geological model was transformed into a petrophysical one where to each layer we allocated the corresponding P-wave velocity and density values. Where found appropriate on the basis of the geological model, the horizontal gradients of the elastic and density properties were also indicated within the layers.

The geological—petrophysical models were converted in the next step into a theoretical seismic section, by convolving the corresponding spike-seismogram with a wavelet having rectangular amplitude characteristics in the prescribed frequency-band and a zero phase shift. The seismic section obtained should be considered as the model of an ideally processed seismic material, after true amplitude recovery, wave-shaping and a drastic reduction of the multiples. Generally, if not otherwise mentioned, diffractions have not been included since it has been found that they play a negligible role in the case of the structures studied.

The seismic model sections derived from the geological—petrophysical models were then entered as inputs to the Pseudo-Acoustic Log (PAL) program package where they re-appeared at the output as reconstructed petrophysical

models in the given frequency band (GOGONENKOV et al. 1980). The PAL sections were computed both with and without using the low-frequency constituents of the input models.

3. Modelling results

The carbonate reefs associated with the anticlinal structures of the Volga–Uralian oil and gas province were modelled on the basis of the geological–petrophysical conditions of the Il'men' site of the Kuibyshev–Volga region (S. E. rim of the Mukhanovo–Erokhovski depression). A preliminary geological–petrophysical section and the vertical distribution of the velocities and densities are shown in *Fig. 1*. The section contains lower and middle Carboniferous deposits, the high-velocity carbonate formations enclose two terrigeneous* complexes forming the main acoustic inhomogeneities: the Vereiski of about 90 m thickness, and the Tarusa of about 15 m thickness. The Vereiski formation is an alternating sandstone/shale sequence, it is relatively poorly differentiated as regards velocities and highly differentiated as regards densities. The thickness of the individual layers fluctuates between 3 and 15 m. The Tarusa Formation consists of shales. Within the carbonate formation the large acoustic inhomogeneities are due to nonuniformly distributed shaly limestone interbeddings of 3–10 m thickness.

The spatial model was constructed on the basis of the data of 5 wells (including the sonic- and gamma—gamma log from the Il'men'–4 well). Results of the high-resolution seismic survey (up to 100 Hz) of the Central Geophysical Expedition were also utilized. The constructed model reveals a reef structure in the Serpukhov stage, located on a small-amplitude uplift. The nucleus of the structure consists of high-density carbonates, joined at the flanks by more shaly differentiations. The complex is overlain by an anticlinal structure within which oil has been found in the upper part of the Bashkirian, in one of the sand layers of the Vereiski Formation, and at the bottom of the Kashira. The petrophysical anomalies associated with these accumulations are small, they only cause a decrease of some 4–6 per cent in the acoustic impedance of the oil-containing layers. Dips and curvatures of the boundaries are also small, 0.5–1.5°.

In this region, the seismic method has to solve the following geological problems (besides the traditional task of mapping the reef body):

a) A general lithologic division of the section into terrigeneous and carbonate layers.

b) Detection of the anomalies due to the presence of hydrocarbons and delineation of the oil-bearing intervals in the Bashkirian, Vereiski and Kashirian horizons.

c) Further subdivision of the Vereiski terrigeneous stratum, tracing of the sand layers.

---

* The translation follows the author's terminology by using "terrigeneous" instead of "clastic" (Editor)
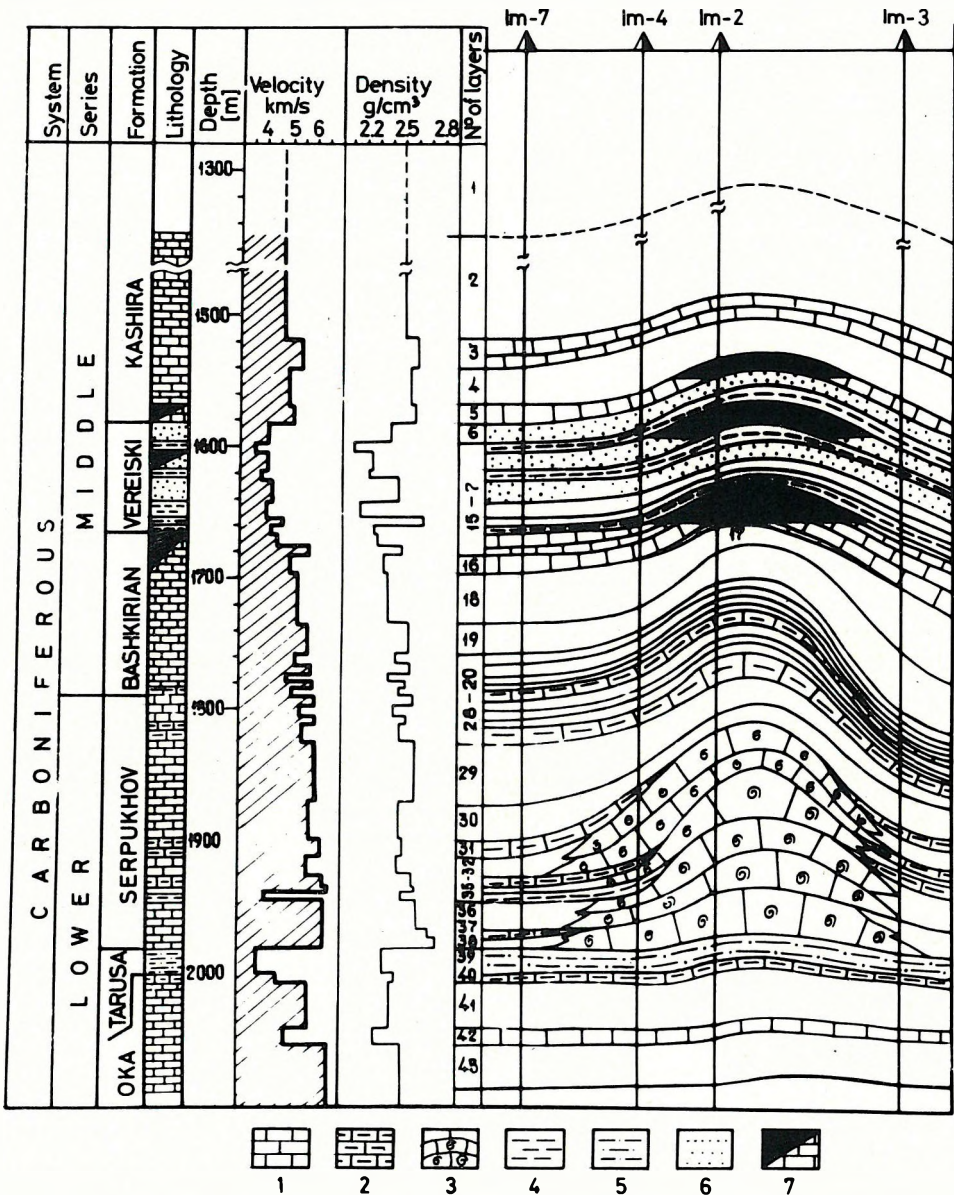
Fig. 1. Geological—petrophysical model of the Il'men' oil field (horizontal scale compressed 1 : 5) 1–3 — limestones: shaly (2); organic (3); 4 — shales; 5 — aleurolites; 6 — sandstone; 7 — oil deposits

1. ábra. Az Il'men' olajmező földtani—kőzetfizikai modellje (a horizontális lépték 1 : 5 arányban összenyomva) 1–3 — mészkő: palás (2), szerves (3); 4 — pala; 5 — aleurolit; 6 — homokkő; 7 — kőolaj telepek

Рис. 1. Геолого-петрофизическая модель разреза Ильменевского месторождения. 1—3 — Известняки: глинистые (2), органогенные (3); 4 — глины; 5 — алевролиты; 6 — песчаники; 7 — залежи нефти.

d) Tracing the facies changes before and after the reef where the shaly limestones change into the dense organic limestone constituting the nucleus of the reef.

e) Mapping the roofs of the reef bodies.

Theoretical seismic time sections, obtained from the above-discussed geologic model, are shown in *Figs. 2.* and *3,* for oil and gas traps and for two frequency bands. The 15–40 Hz band corresponds to the real possibilities of the state of the art, while the 20–110 Hz band is just intended to call attention to the potentialities of the seismic method.

Comparison of the time sections clearly illustrates the increased resolving power of the seismic technique for a wider frequency band. The sections clearly show the anticlinal crest connected with the carbonate structure, the structural details however appear rather different in the different spectral ranges. It seem practically impossible to infer any conclusions on the distribution of the material composition on the basis of the time sections. The oil accumulations do not cause any visible effects on the dynamics of the waves.

The same figures also present the pseudo-acoustic transformations of the corresponding time sections in two variants: with and without utilizing the low-frequency components of the seismic traces. In the display of the PAL results the isolines correspond to equal acoustic impedance values, the actual values being indicated by the density of the hachures. Special attention should be paid to the proper selection of the shades since in the present version of the SHAD-CON program only 5–6 different gradations can be generated; this is obviously not enough to describe the intricate distribution of the material parameters in a wide frequency range. Consequently, the boundaries between the different tones should specially be chosen to allow that the most important acoustic inhomogeneities be clearly separated on the display by visual contrasts between different tones. The problem, and the methodology of the selection of tones should be clear from the analysis presented in *Fig. 4.* The figure shows the original distribution of the acoustic impedances and the pseudo-acoustic logs computed from different frequency bands of a model trace, located at Well No. 4. In the original acoustic impedance curve the blackened parts indicate the change in the acoustic impedance where the formation-water is substituted by oil (and gas, as well) in the potential reservoirs. If we trace this change across the finite-bandwidth seismic model, the boundaries between the different tones have to be chosen such that the transition should coincide with the zones of changes in the formation properties. Obviously, even the visualization of the oil-bearing zones alone would require all possible tones (attaching a single tone to each productive interbedding). Of course, this kind of display would be for from optimal for the illumination of the rest of the geological problems. To circumvent this difficulty, we tried to find another way to select the tones. It goes without saying that this selection was not optimal in each case. The final solution of this question is anticipated from the use of colour plotters having at least 15–20 gradations of colour.
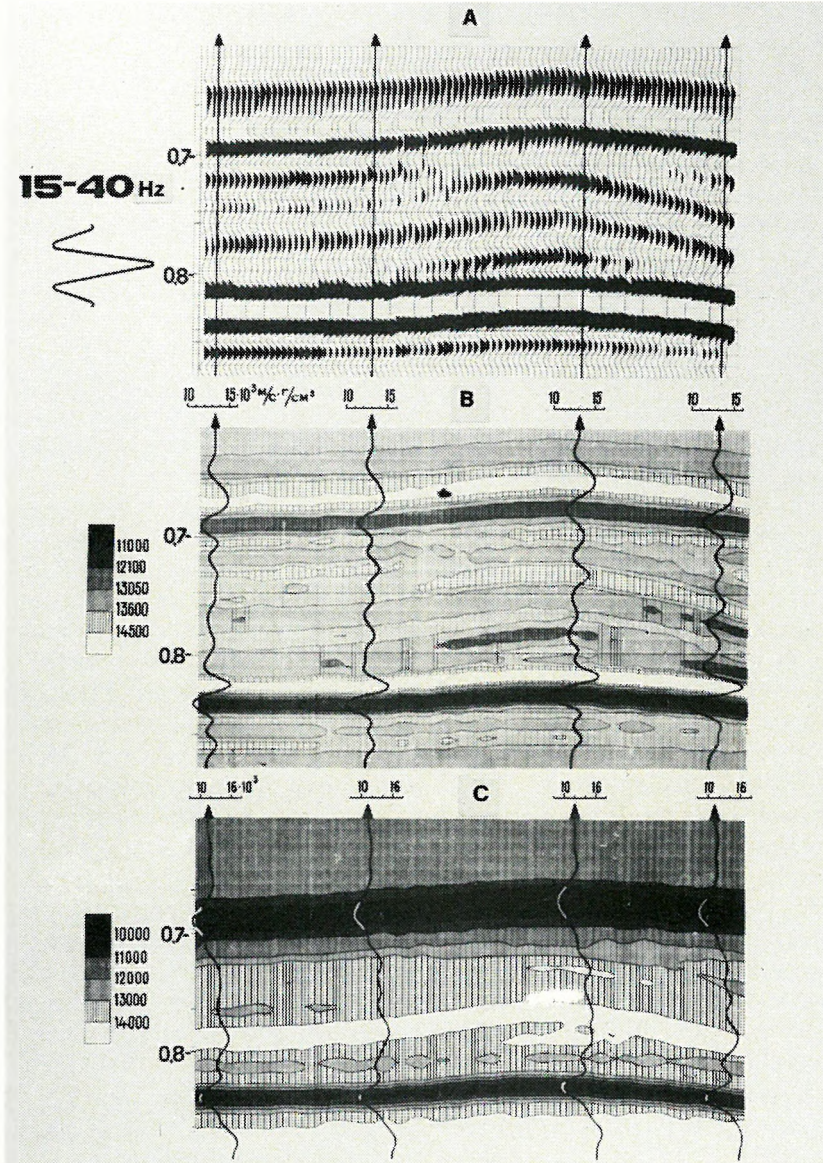
Fig. 2. Comparison of the synthetic time section (A) with the pseudo-acoustic log without (B) and with (C) low-frequency components, for the 15–40 Hz band

2. ábra. A szintetikus időszelvény (A) összehasonlítása a pszeudo-akusztikus komponensek nélkül (B) és azokkal együtt (C) a 15–40 frekvenciasávban

Рис. 2. Сопоставление синтетического временного разреза (А) с разрезами ПАК без введения низкочастотной составляющей (В) и с ее учетом (С) на частотах 15–40 Гц.
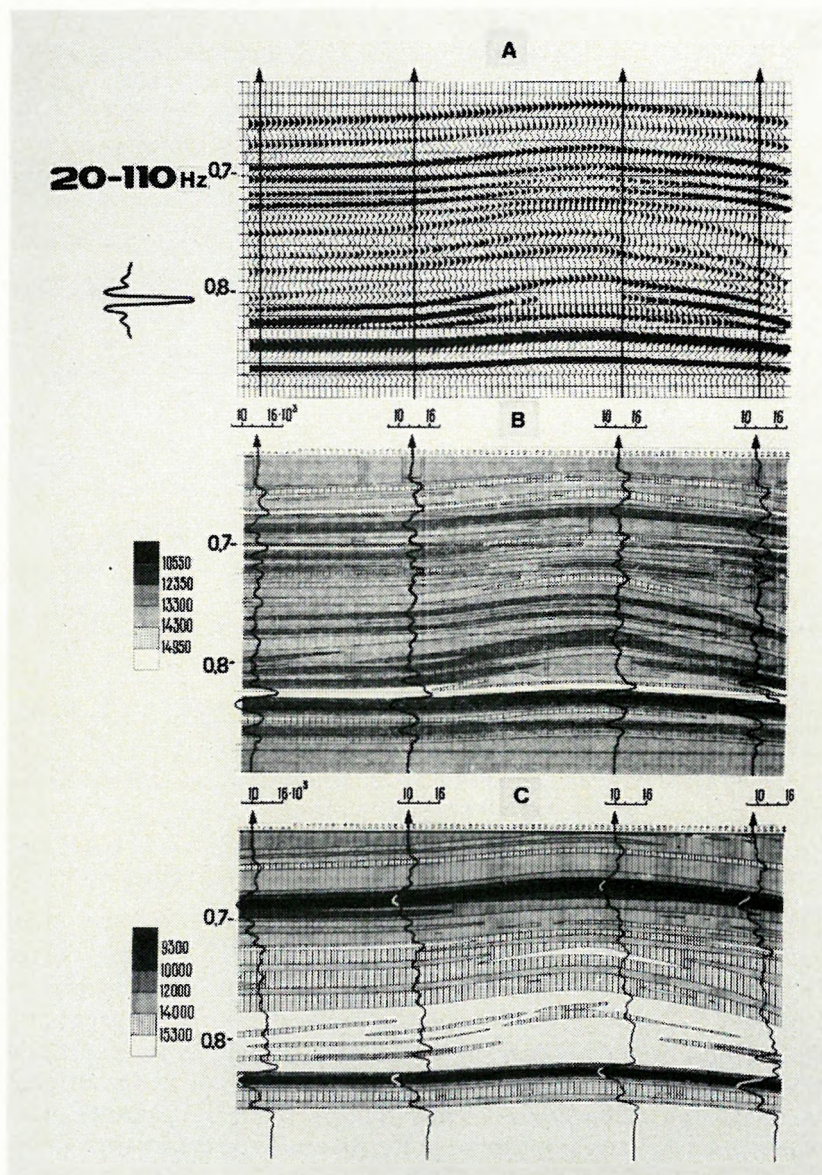
Fig. 3. Comparison of the synthetic time section (A) with the PAL section for the 20–110 Hz spectral range. B and C as in Fig. 2

3. ábra. A szintetikus időszelvény (A) összehasonlítása a pszeudo-akusztikus karotázs szelvénnyel a 20–110 Hz frekvenciasávban. B és C mint a 2. ábrán

Рис. 3. Сопоставление синтетического временного разреза (А) с разрезами ПАК на частотах 20–110 Гц. В и С см. на рис. 2

The pseudo-acoustic sections of Figs. 2 and 3 were displayed by using gradations determined as described above. To facilitate the analysis, four original PAL curves are also superimposed on the sections. Let us first consider the sections constructed without low-frequency components. In order to better understand the following conclusions, it is suggested that simultaneously consideration be given to comparing the curves in Fig. 4. In addition, comparison of the pseudo-acoustic sections should also be done with reference to Fig. 4. where the mutual correspondence of the anomalies can easily be checked.
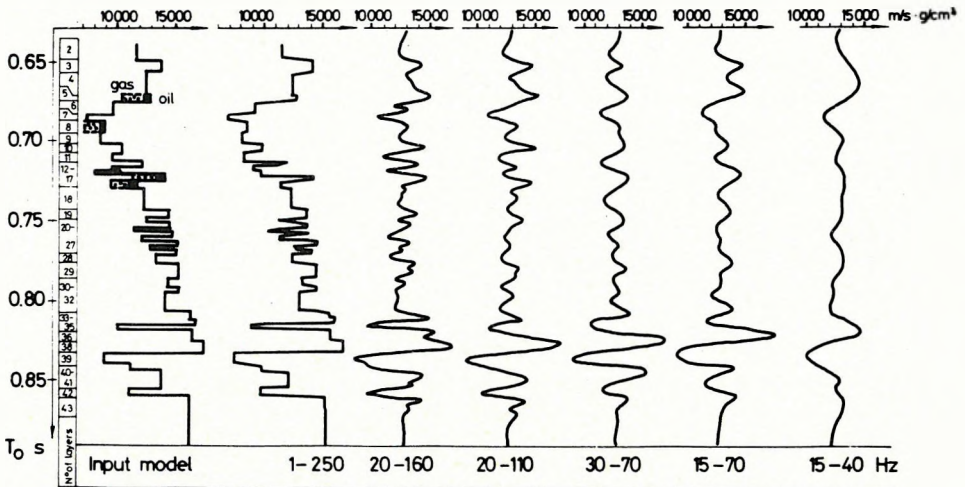

Fig. 4. Comparison of the PAL traces (computed for the Il'men'—4 well) in different frequency bands, without low-fequency components

4. ábra. Az Il'men'—4 sz. fúrásra számított pszeudo-akusztikus karotázs csatornáinak összehasonlítása különböző frekvenciasávokban az alacsonyfrekvenciás komponensek nélkül

Рис. 4. Сопоставление трасс ПАК в опорной точке (скв. 4 — Ильменевская) на разных фильтрациях без низкочастотной составляющей

The PAL section in the narrowest frequency band of 15–40 Hz (Fig. 2) cannot be used except for roughly solving Proble~ :), i.e. for separating the terrigeneous formation. No other problems can be solved because of the limited resolution of the display. Also, it should be noted that, in this particular case the PAL section provides erroneous information about the presence of a thick zone of decreased acoustic impedance in the centre of the organic structure. The suggested thickness of the Vereiski terrigeneous deposit is also misleading.

The section constructed in the 15–70 Hz band yields more definite information. From among the problems listed a), d) and e) can be solved; the effect of the thin deposits is still small and we cannot trace the sand layer in the Vereiski Formation. An essential difference will be found if we consider Fig. 3 constructed from the 20–110 Hz band. All five problems can be solved on the basis of this section. Let us elaborate only one of them, the indication of the small effects due to the oil traps. The deposit in the Kashira limestone presents itself with

a decrease of the acoustic impedance of the first high-velocity layer overlying the Vereiski at 0.67 s. The deposit in the sandstones of the Vereiski horizon also appears with an impedance decrease in the cap of the structure, at 0.685–0.695 s. The most clear-cut anomaly belongs to the Bashkirian deposit, encircled by the 12,500 m/s · g/cm³ isoline at 0.71 s.

The pseudo-acoustic section constructed from the 20–160 Hz band does not contribute too much to the previous one. The sequences of thin beds can be a little bit better separated, it is easier to trace the oil deposit in the sands of the Vereiski horizon while, on the other hand, the quality of the productive Kashira and Bashkirian layers deteriorates.

As for the differences between the pseudo-acoustic sections constructed with and without supplementary low-frequency information, respectively, it should be noted that the incorporation of the low frequencies resulted in a more detailed lithologic differentation of the layers, and in an important subdivision of the section into intervals of various thickness having different interval velocities (impedances). As the Vereiski terrigeneous formation thins out there clearly appears a zone of increased velocity (impedance) in the reef body and in the underlying carbonates. At the same time, some tiny structural details become less evident since now they are superimposed on a significant background of the velocity increase, recovered from the low-frequency components. For example, in the 20–110 Hz section it is quite difficult to interpret the effect of the deposits. Only the deposit within the Vereiski sandstones reveals itself by increasing the thickness of the low-velocity layer. No other deposit can be traced. Evidently, in such cases where the explored anomalies are small compared with the amplitudes of the low-frequency effects, it could be meaningful to construct and analyse a section without low frequencies.

It is very important to observe that the introduction of the low-frequency components is also helpful in the quantitative estimation of the petrophysical parameters. The accuracy of this estimation will be the larger, the higher the upper cut-off frequency in the seismic spectrum. In order to illustrate this statement we computed the mean square deviation of the generated model from the original one, both for the whole spectrum and without the low-frequency components. The results are shown in *Table I*.

Table I.

Mean square errors (σ) of the PAL values

Cut-off frequency Hz	$\sigma(V)$ [m/s]		$\sigma(V\rho)$ [m/s · g/cm³]	
	with low-frequency components	without low-frequency components	with low-frequency components	without low-frequency components
15– 40	530	960	1380	2512
30– 70	500	880	1300	2297
15– 70	470	870	1220	2268
20–110	370	900	960	2363
20–160	350	845	900	2197

It can be seen that in the models where the low-frequency components had been included the mean square errors are relatively small and they fruther decrease significantly with increasing bandwidth. If the low-frequency components are omitted the error abruptly jumps and depends on the spectral bandwidth.

The model considered above is an example where it is extremely difficult to detect the anomaly due to the deposit, for this effect is 5–8-times weaker than that due to the lithological differentiation in the section. Let us also consider a more simple example—when the objects studied are deposits containing gas rather than oil. In this case the acoustic impedance mismatch abruptly increases to 15–20%, instead of its previous value of 3–5%. *Figures 5* and *6* show models constructed for the 15–40 Hz and 20–110 Hz frequency bands, productive layers being assumed as gas-bearing. It is immediately seen even on the synthetic seismic section that the wave patterns have undergone a significant change in the intervals of the deposits. There is a change in the intensity of the seismic records, there appeared the classical "bright spot", especially clearly seen at low frequencies. The correlation of the reflections in the Vereiski Formation has deteriorated. The velocity decrease in the deposits has led to a flattening out of the arch of the structure so that the amplitude of the structure in the Tarusa horizon has become barely observable. Note that on the PAL sections— both with and without the low-frequency components—we can always clearly see the anomalies associated with the reservoirs. The 15–40 Hz range, however, is obviously insufficient for an accurate localization of these deposits, whereas the 20–110 Hz range efficiently maps all of them individually, determines their spactial dimensions and configuration. Let us also add that while in the PAL section with "oil deposits" special care had to be taken for the proper selection of the gradation of the hachure in order to enhance the desired effects, in the case of "gas" an arbitrary distribution of the shades has been used and the anomalies are nonetheless clearly seen.

4. Conclusions

In summary, the analysis of the model result suggests a number of general principles concerning the proper interpretation of the PAL sections:

a) The extension of the frequency spectrum of the signals to be transformed plays a key role in the correct geological interpretation of the PAL data. For any actual geological problem and for any set of seismic conditions we can formulate the requirements concerning the frequency bandwidth. These requirements can be determined by means of modelling as in the study described above.

b) If the object studied has extreme acoustic impedance properties in the analysed interval (this interval should contain at least 2.5–3.0 periods of the dominant frequency) and the variations of the acoustic properties through the object's boundary are much stronger than the differentiations in the distant parts of the section, the pseudo-acoustic construction would reliably delineate
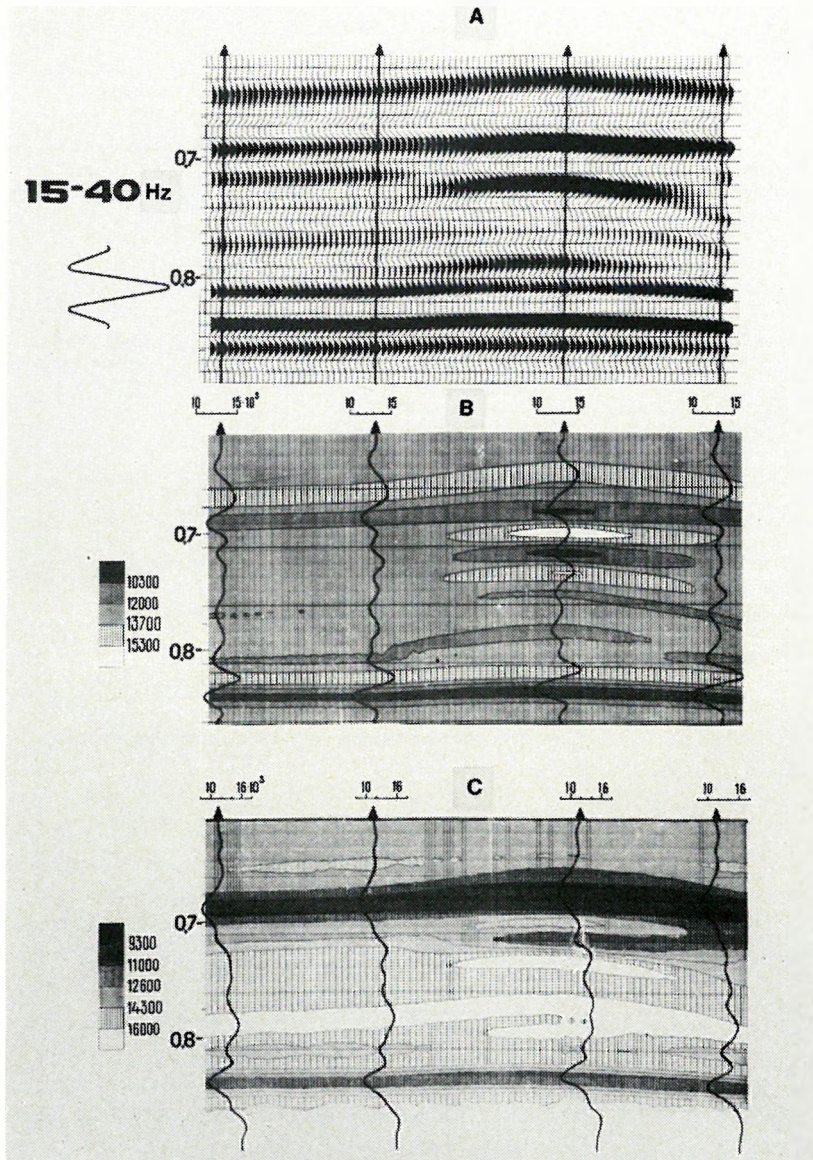
Fig. 5. Comparison of the synthetic time section (A) with the PAL section for the 15–40 Hz spectral range, in the presence of a gas deposit. B and C as in Fig. 2

5. ábra. A szintetikus időszelvény (A) összehasonlítása a pszeudo-akusztikus karotázs szelvénnyel a 15–40 Hz frekvenciasávban, gáztelep esetén. B és C mint a 2. ábrán

Рис. 5. Сопоставление синтетического временного разреза (A) с разрезами ПАК на частотах 15–40 Гц с залежью газа. B и C см. на рис. 2
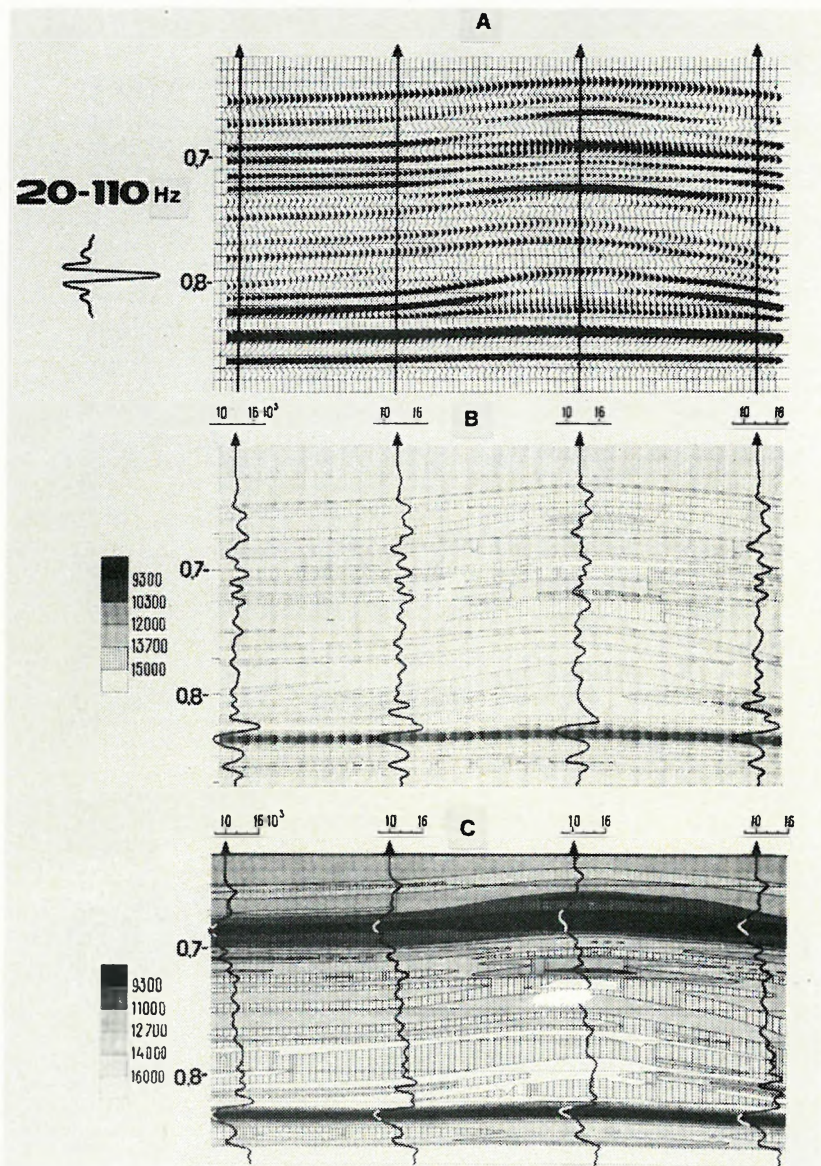
Fig. 6. Comparison of the synthetic time section (A) with the PAL section for the 20–110 Hz band, in the presence of a gas deposit. B and C as in Fig. 2

6. ábra. A szintetikus időszelvény (A) összehasonlítása a pszeudo-akusztikus karotázs szelvénnyel a 20–110 Hz frekvenciasávban, gáztelep esetén. B és C mint a 2. ábrán

Рис. 6. Сопоставление синтетического временного разреза (A) с разрезами ПАК на частотах 20–110 Гц с залежью газа. В и С см. на рис. 2

the object and it would clearly show the variations in its material properties. The accuracy of the reconstruction of the original values of the elastic parameters of the study object depends on the ratio of its thickness (in transit time units) and the upper limiting frequency in the signal spectrum. The quantitative estimations of the acoustic impedance will agree with original values only if the condition

$$\frac{1}{f_n} \leq \Delta T = \frac{2h}{V} \tag{1}$$

is valid, where

f_n is the upper limiting frequency in the spectrum of the seismic records;
ΔT is the two-way transit time across the object studied;
h is its thickness;
V is the sound wave propagation velocity in the object.

If Condition (1) is not satisfied, estimations of the material properties will contain substantial errors; however, the spatial location of the target and the general character of the changes of the parameters within this target will be obtained fairly reliably.

c) If the study object is not extremal with regard to its acoustic impedance in the interval analysed, i.e. there is an even more contrasty acoustic inhomogeneity in its immediate neighbourhood, then, if Condition (1) is satisfied both for the study object and for the nearby inhomogeneity, the study object can accurately be mapped and its properties estimated. If Condition (1) does not hold either for the study object or for the more contrasty nearby inhomogeneity, very significant errors could result from estimating the properties, position, form and even the very existence of the target.

d) The absence of the low-frequency components does not complicate, in some cases it even facilitates the detection and mapping of those targets whose two-way time thickness is significantly larger than the lower limiting frequency in the seismic spectrum. In this case, however, no accurate quantitative estimation of the elastic parameters can be given, though the relative change between the properties in the anomalous body and its surroundings can fairly well be estimated.

e) The application of the low-frequency components helps in dividing the section into layers of considerable thickness having different lithology. If Condition (1) is met both for the study object and for the surrounding layers, the elastic properties of the object can quantitatively be determined.

f) If the PAL sections are displayed using impedance isolines, the appropriate selection of the boundaries between different gradations plays a decisive role. Preferably, this selection should be made in advance, in correspondence with the geological problem to be solved and with the expected changes of the material properties. If there are several anomalous objects on the same section, having widely different properties, it could be meaningful to prepare two or more different displays with different gradations of the hachures.

g) The results of analyses of this kind should be compiled to be used as educational materials for a wide circle of seismic interpreters and geologists interesed in the possibilities and limitations of the method of pseudo-acoustic transformation of seismic data.

REFERENCES

BOISSE, S. 1978: Calculation of velocity from seismic reflection amplitude. Geophisysical Prospecting, **26**, 1, pp. 163–174

GARDNER, G. 1974: Synthetic seismics via synthetic logs tells lithology from regular seismics. Oil-Week, **25**, 35, pp. 64–66

GOGONENKOV, G. N., ANTIPIN, YU. G. 1970: Effective models of real thin-layered media (in Russian). Izv. AN SSSR, Ser. Fizika Zemli, **3**, pp. 3–11

GOGONENKOV, G. N., ZAKHAROV, E. T., ÉL'MANOVICH, S. S. 1980: Prediction of the detailed velocity section from seismic data (in Russian). Prikladnaya Geofizika, **97**, pp. 58–72

GOGONENKOV, G. N., PETERSEN, G. N. 1982: Reconstruction of the detailed velocity characteristics from seismic data (the pseudo-acoustic log, in Russian). VNIIOENG, 27, Moscow

LINDSETH, R. O. 1979: Synthetic sonic logs—a process for stratigraphic interpretation. Geophysics, **44**, 1, pp. 3–26

STREET, A. V. 1978: Seislog uses continue to expand. Oil and Gas Journal, **76**, 44, pp. 59-65

G. N. GOGONENKOV, N. D. PAVLOV, V. D. LEVCSENKO, B. I. AGAFONOV

A PSZEUDO-AKUSZTIKUS SZELVÉNYEK SZEIZMIKUS MODELLEZÉSEN ALAPULÓ KIÉRTÉKELÉSI MÓDSZEREI

A cikkben a Volga—Urali olaj- és gázmező földtanilag jellemző területén végzett szeizmikus modelltanulmányt mutatnak be. A számított szintetikus időszelvényeket akusztikus impedancia szelvényekké transzformálják vissza annak érdekében, hogy tanulmányozhassák a pszeudo-akusztikus karotázs alkalmazási lehetőségeit a produktív formációk finom szerkezetének és anyagi jellemzőinek kutatásában.

Az eredményeket elemezve és az eredeti input modellekkel összehasonlítva általános következtetéseket vonnak le, és a pszeudo-akusztikus szelvények megfelelő kiértékelésére vonatkozó előírásokat fogalmaznak meg.

Г. Н. ГОРОНЕНКОВ, Н. Д. ПАВЛОВ, В. Д. ЛЕВЧЕНКО, Б. И. АГАФОНОВ

РАЗРАБОТКА МЕТОДИКИ ИНТЕРПРЕТАЦИИ ПСЕВДОАКУСТИЧЕСКИХ РАЗРЕЗОВ НА ОСНОВЕ ГЕОСЕЙСМИЧЕСКОГО МОДЕЛИРОВАНИЯ

На примере геологической ситуации, типичной для районов Волго—Уральской нефтегазоносной провинции, путем расчетов синтетических временных разрезов и последующего преобразования их в разрезы акустической жесткости демонстрируются возможности методики для изучения детального строения и продуктивных толщ. Анализ полученных результатов и их сопоставление с исходной моделью геофизического разреза позволил сформулировать некоторые принципы интерпретации данных псевдоакустического преобразования.

AUTOMATIC VELOCITY ANALYSIS

Róbert MÄRLE*

A new way is described for the automatic determination of seismic velocities, by means of iterative stacking. The procedure is based on the favourable properties of iterative summation and on some general observations concerning the behaviour of the stacking velocity.

1. Introduction

A novel method is introduced for the automatic determination of the stacking velocity. The basic idea of velocity analyses can always be reduced to a signal detection problem. The algorithm selects that particular value of the velocity for which there is the highest likelihood of signal arrival. The decision about the presence or absence of the signal is made on the basis of statistical hypothesis testing. One has to define and compute a measure S of similarity and to compare it with some prescribed threshold S_0 to see whether it is greater than or less than this threshold. If $S > S_0$ we accept the hypothesis that a signal arrived and we then determine the corresponding velocity. Following NAESS [1979] we propose determining the measure of similarity by means of an iterative stacking technique. This iterative procedure improves the S/N ratio and, consequently, provides an easier way to determine the velocities [NAESS and BRULAND 1979]. Some mathematical properties of the iterative summation method are given in the Appendix.

The final determination of the whole velocity function is carried out by an algorithm based on the properties of the stacking velocity [COCHRAN 1973].

2. Algorithm of iterative stacking

The algorithm should be carried out on the amplitudes belonging to the same time instants of the statically and dynamically corrected CDP traces. Let us introduce the following notations:

a_i' the i-th positive amplitude,
b_j' the j-th negative amplitude,
m number of positive amplitudes,
n number of negative amplitudes,
M fold number.

* Eötvös Loránd Geophysical Institute of Hungary;
  POB 35. Budapest, H-1440

We denote by $S' = S'_+ + S'_-$ the usual stacking where

$$S'_+ = \frac{1}{M} \sum_{i=1}^{m} a'_i$$

$$S'_- = \frac{1}{M} \sum_{j=1}^{n} b'_j$$

(1)

In the next step, let us define the amplitudes a''_i and b''_j as follows:

$$
\begin{array}{llll}
\text{If} & a'_i > S'_+ & \text{then} & a''_i = S'_+ \\
\text{if} & a'_i \leq S'_+ & \text{then} & a''_i = a'_i \\
\text{if} & b'_j < S'_- & \text{then} & b''_j = S'_- \\
\text{if} & b'_j \geq S'_- & \text{then} & b''_j = b'_j
\end{array}
$$

(2)

From these new amplitudes a summation yields the next stacking:

$$S'' = S''_+ + S''_-$$

(3)

where

$$S''_+ = \frac{1}{M} \sum_{i=1}^{m} a''_i$$

$$S''_- = \frac{1}{M} \sum_{j=1}^{n} b''_j$$

(4)

More generally, after the q-th iteration step we have

$$S^{(q)} = S^{(q)}_+ + S^{(q)}_-$$

(5)

with

$$S^{(q)}_+ = \frac{1}{M} \sum_{i=1}^{m} a_i^{(q)}$$

$$S^{(q)}_- = \frac{1}{M} \sum_{j=1}^{n} b_j^{(q)}$$

(6)

The amplitudes $a_i^{(q)}$ and $b_j^{(q)}$ are obtained as follows:

$$
\begin{array}{llll}
\text{If} & a_i^{(p)} > S_+^{(p)} & \text{then} & a_i^{(p+1)} = S_+^{(p)} \\
\text{if} & a_i^{(p)} \leq S_+^{(p)} & \text{then} & a_i^{(p+1)} = a_i^{(p)} \\
\text{if} & b_j^{(p)} < S_-^{(p)} & \text{then} & b_j^{(p+1)} = S_-^{(p)} \\
\text{if} & b_j^{(p)} \geq S_-^{(p)} & \text{then} & b_j^{(p+1)} = b_j^{(p)}
\end{array}
$$

(7)

where $p = 1, 2, \ldots, q - 1$.

The upper index q indicates that the amplitudes have been changed, at most, $(q - 1)$ times. During these changes the amplitudes get increasingly closer to each other and the S/N ratio improves.

3. Algorithm of velocity determination

The task of velocity determination is reduced to a signal detection problem. On borrowing terms from statistical signal detection theory, the problem can be rephrased as follows:

Signal detection is basically a problem of statistical hypothesis testing. We have to choose between two hypotheses, viz. H_0: no signal present, H_1: signal present. In order to decide between these alternatives we compute a statistics r and compare it with a previously given threshold r_0. For $r > r_0$, the hypothesis H_1 is accepted. (For details see HELSTROM 1968).

In the case of velocity analysis the statistics is provided by the similarity function $S(t_0, v)$. If $S(t_0, v) \geqq S_0$ we accept the hypothesis H_1, if $S(t_0, v) < S_0$, we accept H_0. The choice of the threshold value S_0 will be dealt with in the Appendix.

Obviously, the greater the value of $S(t_0, v)$, the greater likelihood we have for signal arrival.

Consequently, in order to find those values of t for which we receive a signal, and to determine the corresponding velocities, we have to select all local maxima of the $S(t_0, v)$ function that are greater than some prescribed S_0.

In the conventional velocity spectra interpretation we look for the local maxima of the following similarity function:

$$S(t_0, v) = \frac{\sum\limits_{i=1}^{N} \left(\sum\limits_{j=1}^{M} a_{ij} \right)^2}{\sum\limits_{i=1}^{N} \sum\limits_{j=1}^{M} a_{ij}^2} \tag{8}$$

where M is the fold number, N the length of the time gate [TANER and KOEHLER 1969]. Equation (8) defines, obviously, the energy of the stacked trace divided by the average of the energies of the original CDP traces. Because of the favourable properties of iterative stacking, if we use in the numerator of the r.h.s. of (8) M-times the value of the iterative stack rather than the conventional sum $\sum a_{ij}$, the local maxima of the function $S(t_0, v)$ would become sharper, i.e. better recognizable both visually and automatically.

The main idea of the algorithm is that the velocity values will be sought only within a quite wide, though definite range, being characteristic to the field material. The local maxima of the function $S(t_0, v)$ will be selected so that the resulting velocity function should satisfy the following criteria [COCHRAN 1973].

1. In order to grant a reasonable accuracy in the estimation of the interval velocities there should be at least some prescribed lapse (say 100 ms) between subsequent reflections.

2. The interval velocities should change between physically plausible limits (e.g. not less than 1500 m/s and not greater than 10,000 m/s, the boundaries being dependent on the study site).

3. No reflection can be expected unless there is at least 2% difference between the interval velocities.

4. If for any reflection arrival belonging to the two-way time T_0 there appears another one around the time $2T_0$, having approximately the same velocity, this latter one should be considered as a multiple.

Of course, besides meeting all the above criteria, the local maximum should also exceed the prescribed threshold. The exact value of this threshold strongly depends on the number of iterations in the stacking process.

The flow-chart of the algorithm is shown in *Fig. 1*.

4. Practical examples

The following examples refer to two separate time sections, the S/N ratio on the first section is significantly less than on the second one.

Figs. 2 and 3 show the velocity functions determined at two CDP points of the first section. The dashed line denotes the conventionally computed and interpreted velocity function, the solid line the automatically computed one. In *Figs.* 4 and 5 the automatic velocity analysis results are presented, by solid lines for the second section, the thresholds being 0.05 and 0.3 for Figs. 4 and 5, respectively. Dashed lines denote the manual interpretation of the velocity spectra results by two independent geophysicists.

Finally, the last two Figures provide a comparison between the second sections processed according to the conventionally determined (*Fig. 6*), and the automatically determined *(Fig. 7)* velocity functions.

The results obtained thus far have proven the reliability of the proposed method.
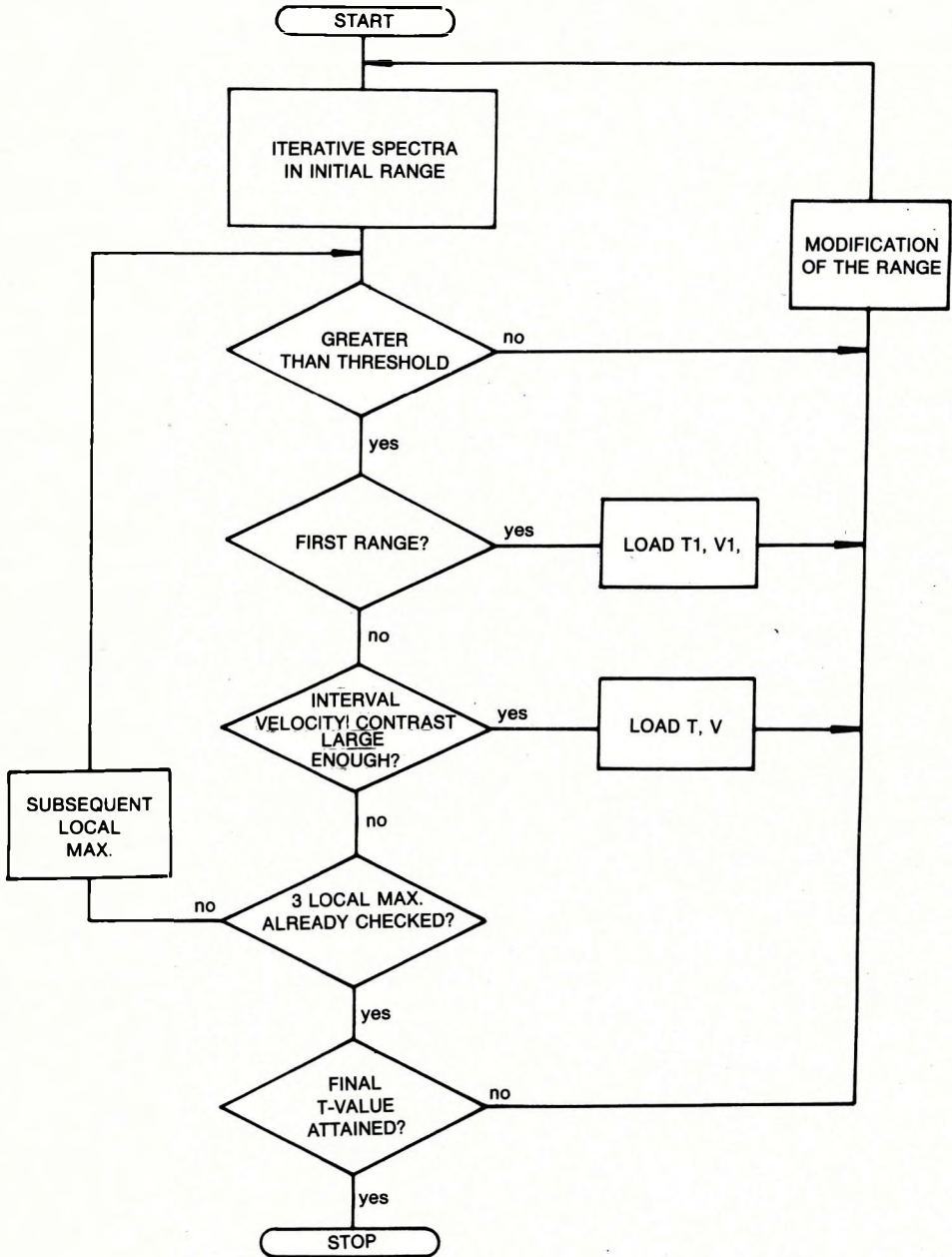
Acknowledgement

Fig. 1. Block diagram of the automatic velocity determination algorithm

1. ábra. Az automatikus sebességmeghatározás algoritmusának blokkvázlata

Puc. 1. Блок-схема алгоритма автоматического определения скорости

stacking velocity

1500 2000   3000   4000   (m/s)
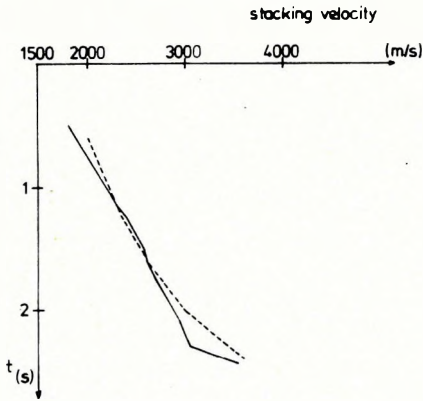
1—

2—

t (s)

Fig. 2. Velocity functions obtained by constant velocity stack (dashed line) and by the new automatic velocity determination (continuous line) for part I. of the profile

2. ábra. Állandó sebességű összegzéssel (szaggatott vonal) és az új automatikus sebességszámító eljárással (folyamatos vonal) meghatározott sebességfüggvény (a szelvény I. szakaszára)

Puc. 2. Скоростные функции, полученные в результате накопления с постоянной скоростью (показанные пунктиром) и применения нового способа для автоматического определения скорости (показанные сплошной линией) для участка I профиля
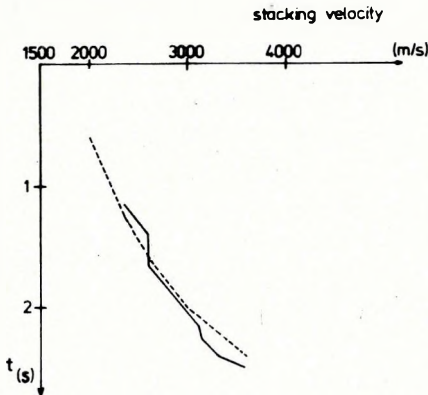
stacking velocity

1500 2000   3000   4000   (m/s)

1—

2—

t (s)

Fig. 3. Velocity functions obtained by constant velocity stack (dashed line) and by the new automatic velocity determination (continuous line) for part II. of the profile

3. ábra. Állandó sebességű összegzéssel (szaggatott vonal) és az új automatikus sebességszámító eljárással (folyamatos vonal) meghatározott sebességfüggvény (a szelvény II. szakaszára)

Puc. 3. Скоростные функции, полученные в результате накопления с постоянной скоростью (показанная пунктиром) и применения нового способа для автоматического определения скорости (показанная сплошной линией) для участка II профиля
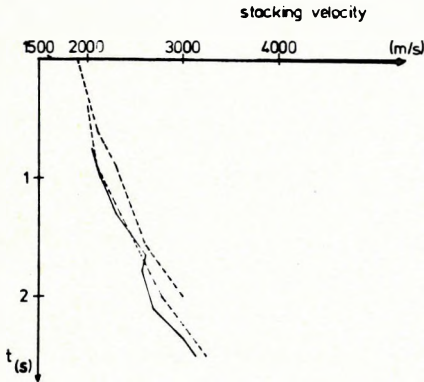
stacking velocity

1500 2000   3000   4000   (m/s)

1

2

t (s)

Fig. 4. Velocity functions obtained by two different interpreters using constant velocity stack (dashed lines) and by automatic velocity determination (continuous line). In automatic computation the threshold: 0.05

4. ábra. Állandó sebességű összegzéssel, két különböző kiértékelő által (szaggatott vonal), és az automatikus sebességmeghatározó eljárással (folyamatos vonal) meghatározott sebességfüggvény.
Az automatikus sebességmeghatározásnál alkalmazott küszöbérték: 0,05

Рис. 4. Скоростные функции, полученные двумя разными интерпретаторами при накоплении с постоянной скоростью (показанная пунктиром), и в результате использования способа автоматического определения скорости (показанная сплошной линией).
Значение порога при автоматическом определении скорости составляет 0,05
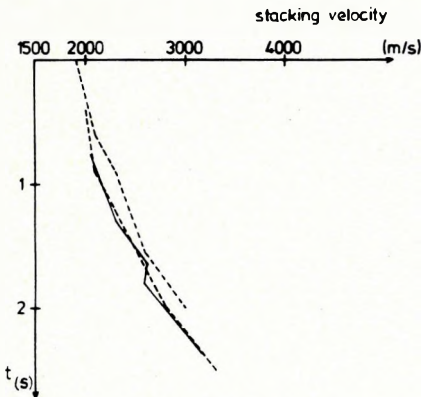
stacking velocity

1500 2000   3000   4000   (m/s)

1

2

t (s)

Fig. 5. Velocity functions obtained by two different interpreters using constant velocity stack (dashed lines) and by automatic velocity determination (continuous line). In automatic computation the threshold: 0.3

5. ábra. Állandó sebességű összegzéssel, két különböző kiértékelő által (szaggatott vonal), és az automatikus sebességmeghatározó eljárással (folyamatos vonal) meghatározott sebességfüggvény.
Az automatikus sebességmeghatározásnál alkalmazott küszöbérték: 0,3

Рис. 5. Скоростные функции, полученные двумя разными интерпретаторами при накоплении с постоянной скоростью (показанная пунктиром), и в результате использования способа автоматического определения скорости (показанная сплошной линией).
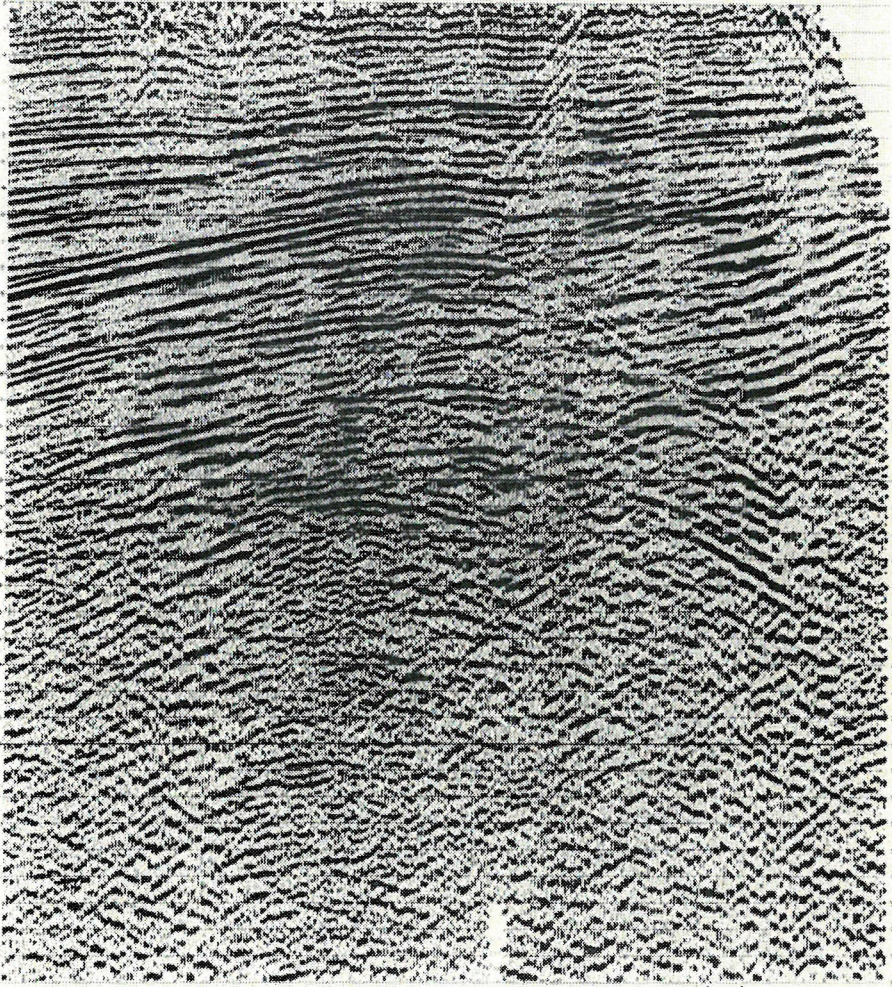
Fig. 6. Seismic time section using CVS velocity functions for processing

6. ábra. Állandó sebességű összegzéssel meghatározott sebességfüggvény alkalmazásával feldolgozott időszelvény

Рис. 6. Временный разрез, обработанный с применением скоростной функции, определенной путем накопления с постоянной скоростью
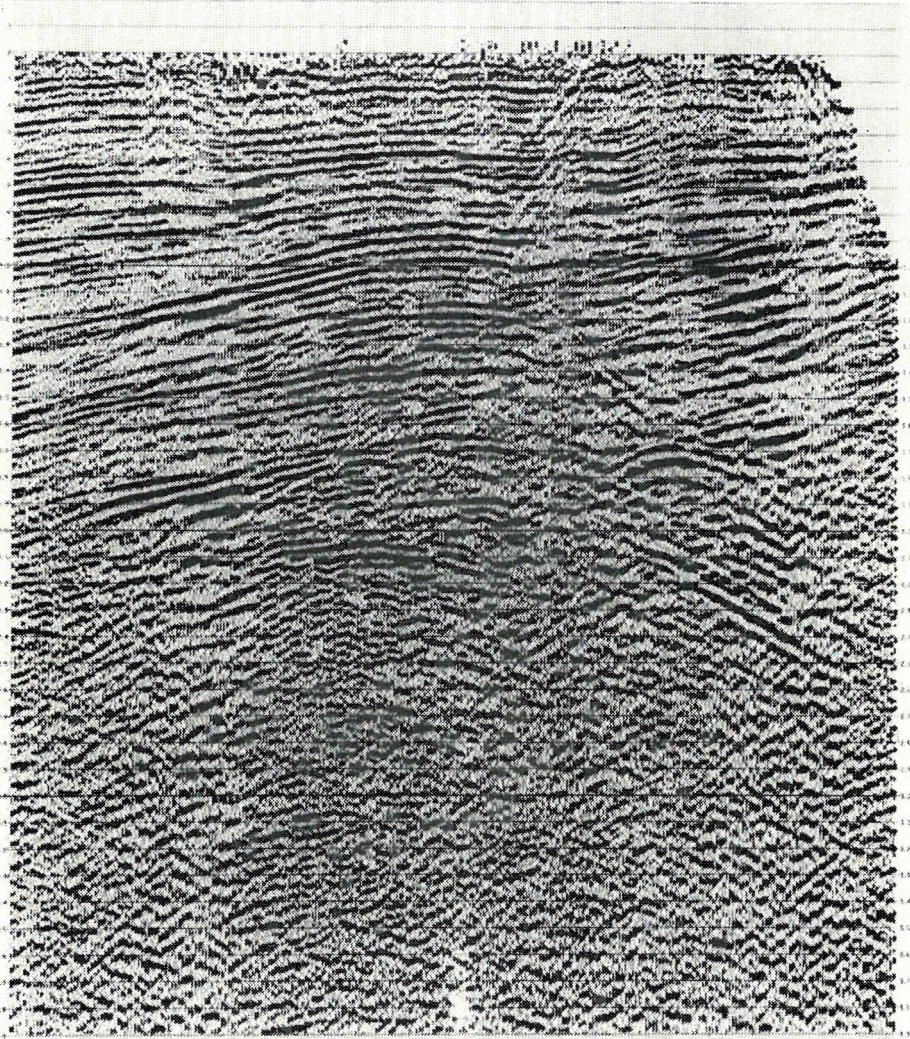
Fig. 7. Seismic time section using the velocity functions of the automatic velocity determination for processing

7. ábra. Automatikus sebességmeghatározó eljárással kapott sebességfüggvénnyel feldolgozott időszelvény

Рис. 7. Временной разрез, обработанный с применением скоростной функции, полученный способом автоматического определения скорости

Appendix

Basic properties of iterative stacking

In what follows we shall derive the expectance and scatter of the iterative stacking for a very simple case when only noise is present. It is hoped that this simple example will suffice to demonstrate the advantages of the method compared with conventional stacking.

Suppose we are given N traces each containing only a binomially distributed binary noise assuming the values of $+1$ or -1. We proceed to show that if the probability p (of the positive value) is near to $1/2$, after two iterations the scatter of the iterative stack will be less than that of the conventional stack.

Suppose that from among the N traces there are k "$+1$"-s and $(N-k)$ "-1"-s. The probability of this is $\binom{N}{k} p^k q^{N-k}$ $(p+q=1)$.

The value of the conventional stack is, for this case, $\dfrac{2k}{N} - 1$, its expectance being

$$M(S) = \sum_{k=0}^{N} \left(\frac{2k}{N} - 1 \right) \binom{N}{k} p^k q^{N-k} = 2p - 1$$

with a scatter

$$D^2(S) = \sum_{k=0}^{N} \left(\frac{2k}{N} - 1 \right)^2 \binom{N}{k} p^k q^{N-k} - (2p-1)^2 = \frac{4pq}{N}$$

Let us now consider the evolution of the iterative stack:

$$S_+^{(0)} = \frac{k}{N} \qquad S_-^{(0)} = - \frac{N-k}{N}$$

$$a_i^{(1)} = \frac{k}{N} \qquad b_j^{(1)} = \frac{N-k}{N}$$

$$S_+^{(1)} = \frac{k^2}{N^2} \qquad S_-^{(1)} = - \frac{(N-k)^2}{N^2}$$

$$a_i^{(2)} = \frac{k^2}{N^2} \qquad b_j^{(2)} = - \frac{(N-k)^2}{N^2}$$

$$S_+^{(2)} = \frac{k^3}{N^3} \qquad S_-^{(2)} = - \frac{(N-k)^3}{N^3}$$

$$S^{(3)} = \frac{k^3 - (N-k)^3}{N^3} = \frac{2k^3 + 3N^2 k - 3Nk^2 - N^3}{N^3}$$

The expectance of the above expression is

$$M(S^{(3)}) = \sum_{k=0}^{N} \frac{2k^3 + 3N^2k - 3Nk^2 - N^3}{N^3} \binom{N}{k} p^k q^{N-k} =$$

$$= 2p^3 + \frac{6p^2q}{N} + 3pq - \frac{3pq}{N} - 1 + O(N^{-2})$$

and similarly, after some awkward but elementary algebra,

$$D^2(S^{(3)}) = \frac{9pq + 36(p^3q^3 - p^2q^2)}{N} + O(N^{-2})$$

Consequently, $D^2(S^{(3)}) < D^2(S)$ if $1/4 < p < 3/4$.

In other words, in all practical cases the S/N improvement in the iterative stack will be faster than in conventional summation.

In the selection of the threshold we recall the well-known fact that it is very unlikely that no signal will be found if the magnitude of the statistics is greater than three times the scatter. For example, if $p = 1/2$, and $N = 12$, the threshold 0.05 seems appropriate. It is not worth while to select a much larger threshold for this would increase the probability of missing some of the signals that have actually arrived.

REFERENCES

COCHRAN, M. D. 1973: Seismic signal detection using sign bit. Geophysics, **38**, 6, pp. 1042–1052
HELSTROM, C. W. 1968: Statistical theory of signal detection. Pergamon Press, New York
NAESS, O. E. 1979: Superstack — an iterative stacking algorithm. Geophysical Prospecting, **27**, 1, pp. 16–28
NAESS, O. E., BRULAND, L. 1981: Velocity analysis using iterative stacking. Geophysical Prospecting, **29**, 1, pp. 1–20
TANER, M. T., KOEHLER, F. 1969: Velocity spectra — digital computer derivation and applications of velocity functions. Geophysics, **34**, 6, pp. 859–881

MÄRLE RÓBERT

AUTOMATIKUS SEBESSÉGANALÍZIS

A dolgozat egy olyan automatikus sebesség meghatározó eljárást ír le, amely iteratív stacking-et használ fel. Az eljárás az iteratív stacking-nek a sebesség meghatározás szempontjából előnyös tulajdonságain és a stacking-sebesség általános jellemzőin alapul.

Р. МЭРЛЕ

АВТОМАТИЧЕСКИЙ АНАЛИЗ СКОРОСТЕЙ

В работе описывается способ автоматического определения скорости, который использует итеративное накапливание. Способ основан на достоинствах итеративного накапливания с точки зрения определения скорости и общих характерискитах скорости накопления.

INTEGRATED INTERPRETATION OF GEOLOGICAL AND GEOPHYSICAL DATA IN OIL AND GAS EXPLORATION AND PROSPECTING

V. Yu. ZAICHENKO*, E. V. KARUS**, E. A. KOZLOV**, V. M. TIKHOMIROV***

The problem of integrated interpretation of geological, geophysical and geochemical data before preparing oil- and gas-exploratory drillings is solved by a sequence of special procedures. Their main steps are: outlining of a region with indications of oil accumulation; quantitative prediction of hydrocarbon potential, estimation of parameters of the reservoirs (size, shape, hydrocarbon content) and selection of sites of exploratory wells.

The performing of the described procedure is based on a specialized package of computer programs which was tested on two hydrocarbon occurrences.

d: oil and gas fields, reserves, computer programs, prediction maps

1. Introduction

At the present time the organizations of the USSR Ministry of Geology apply geophysical methods to delineate and prepare for drilling around 96% of oil and gas prospective structures. The switch-over to digital data acquisition in the main geophysical methods brought a sharp increase in the bulk of annual information, and improved its reliability and geological comprehensiveness. The implementation of digital data processing allowed more complex geological interpretation.

The main difficulties in practical geological interpretation are related to the fact that the traditional visual methods—comparing maps and sections—are unable to provide for high-quality integrated analysis of the geological, geophysical, well-logging, and geochemical data-sets. As a result, at the prospecting stage, the problem is limited to the use of a single relationship—the correlation of hydrocarbon accumulations with anticlines (structural traps), which is usually confirmed in about 30% of the cases. For the same reason, the data of geophysical surveys at the exploration stage are applied even less, usually when selecting sites of the first wells. The subsequent drill sites are selected using maps compiled from the results of exploratory wells.

The presented approach is implemented by using the existing automatic data management systems in the process of exploration for oil and gas to

* USSR Ministry of Geology 4/6 B. Gruzinskaya str. Moscow 123242 USSR
** VNIIgeofizika 22 Chernyshevski str. Moscow 103062 USSR
*** NPO VNIIgeofiziki 5 Kievskoe shosse, Naro-Forminsk, Moscow region, 143300 USSR

manage the process of prospecting for oil and gas regardless of the details of the approach [ARONOV 1977, VOLKOV 1977, KNORING 1977].

2. Geological—geophysical data management systems

A number of organisations of the USSR Ministry of Geology have been engaged in developing the GEOPACK system [KOZLOV–TIKHOMIROV 1979] with the aim of increasing the efficiency of exploration by the more comprehensive use of the accumulated geophysical information. The system involves the realization of the full processing-cycle, as well as independent and integrated interpretation of geological, geophysical, geochemical and other data, including exploitation management decisions.

GEOPACK is a complex of interrelated subsystems with the following main structural elements: *(Fig. 1.)*:
— a set of program packages for different methods: seismic (SEISPACK), gravity (GRAVIPACK), etc.;
— a package of integrated interpretation and management (COMPACK);
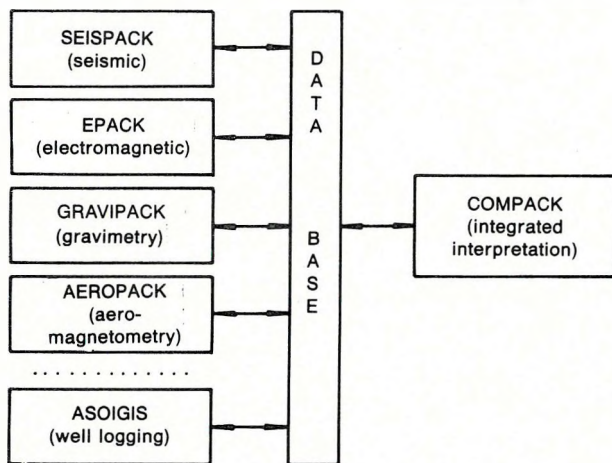— geophysical data base.

Fig. 1. Structure of the GEO-PACK system

1. ábra. A GEOPACK rendszer felépítése

Puc. 1. Структура ГЕОПАКа

The packages process the initial data of each method up to a level of qualitative and quantitative interpretation. The output of results (geophysical and geochemical contour maps, charts, sections, etc.) is stored in the geophysical data base in the form of files on disks and tapes.

The integrated interpretation of the diverse information available is carried out within the COMPACK subsystem. Through the geophysical data base, COMPACK takes in the whole flow of geological/geophysical parameters resulting form the program packages of separate geophysical methods, and produces management decisions.

The COMPACK subsystem can be considered as the software basis of automatic control systems (ACS) currently developed:

EACS — to control exploration within an area, and

PACS — to control prospecting of the located oil and gas traps (reservoirs).

The main tasks performed by the EACS system are:

— selecting promising targets (intervals, structures, zones, etc.);

— the evaluation of the selected target;

— selecting the optimum sites for prospecting wells including the number of wells and their order of succession;

— decision-making concerning stopping or continuing the exploration process;

— making preliminary reserve estimates for the located reservoir before its prospecting.

The PACS system is designed for

— contouring an up-dated structural map of the territory;

— mapping the internal and external oil, gas, and water outlines;

— making a quantitative reserve estimate and appraising its error;

— determining the intensity of further prospecting (the number of rigs to be operated);

— selecting the site of the next well or group of wells;

— determining the number of wells sufficient for prospecting.

The aims of the EACS and PACS systems are reached through solving the following problems which may be reduced to processing of the initial and intermediate files:

(1) construction of a multidimensional matrix of indicators,

(2) selection of a rational set of geophysical methods,

(3) reduction of the initial data set,

(4) prediction of hydrocarbon potentials,

(5) integrated evaluation of all parameters,

(6) planning of exploration drillings,

(7) planning of prospecting drillings.

The structure of the COMPACK subsystem is presented in *Fig. 2*. The formulation of these problems and the approaches to their solution can be reduced to the following:

1. The problem of generating an integrated table of the initial data consists of the collection and systematization of the available geological, geophysical and geochemical data to form a multidimensional matrix of indicators. The problem falls into several subproblems:

1.1 Transformation of qualitative, non-measurable indicators (for instance, colour) in binary codes over a regular or non-regular grid;

1.2 preliminary data processing, switch-over from the non-regular grid to a regular one, and subdivision into blocks. Quantitative, essentially non-continuous fields are corrected using the results of drilling (e.g. faulting);

1.3 preliminary smoothing;

1.4 interpolation of the missing values of indicators;

1.5 Expansion of the matrix of indicators presented by the cumulative table using the spatial properties of scalar-, potential- and encoded qualitative fields. Such qualitative parameters as the squared dip of a horizon, its total and mean curvature, relationship of horizons, and others are used as additional indicators.

2. The selection of a rational set of surface geophysical surveys is made with the aid of the method of conventional correlation capable of estimating the significance of the relationships between groups of indicators. The resulting data file is a table of correlation coefficients that helps in selecting the most efficient set of geological, geophysical and geochemical surveys.
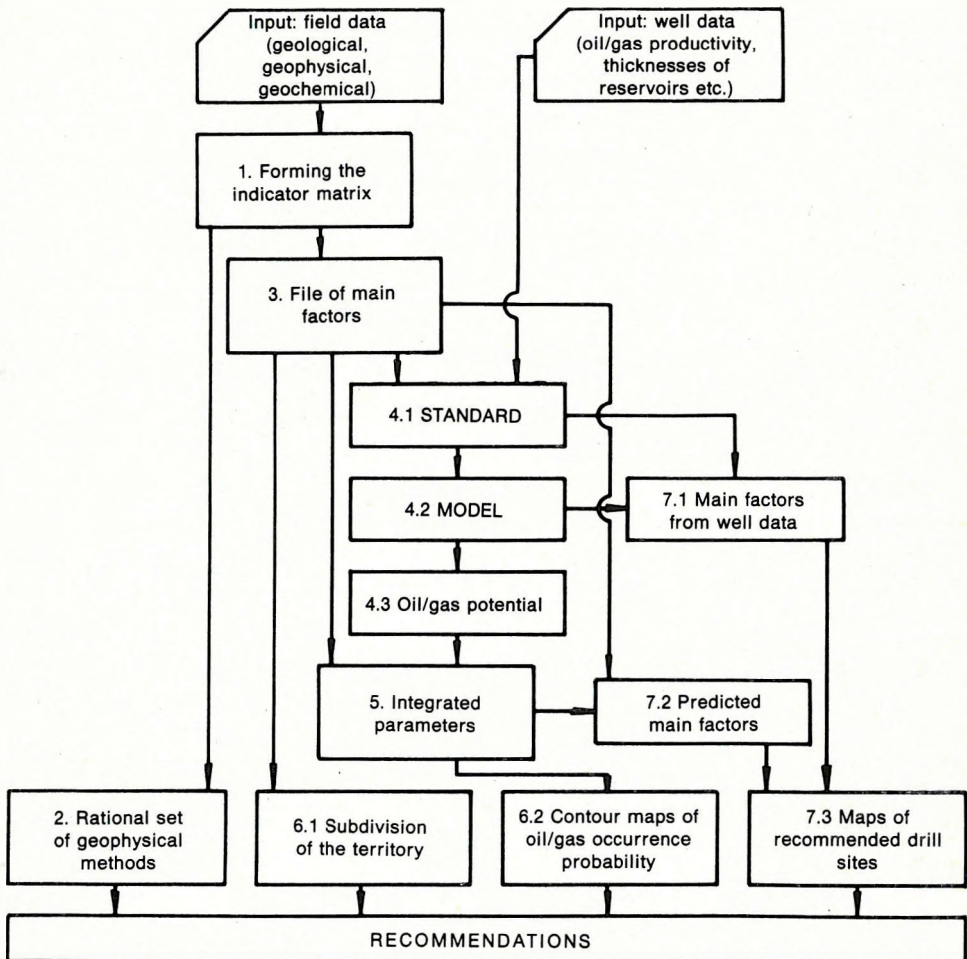

Fig. 2. Flow chart of the COMPACK subsystem

2. ábra. A COMPACK alrendszer blokkdiagramja

Puc. 2. Схема преобразования информации в подсистеме КОМПАК

3. The reduction of the initial indicator matrix generated at stage 1.5 can be accomplished by several different techniques. One of them is the method of main factors which — under favourable conditions — renders possible a quantitative estimation of the factors responsible for the observed anomalies. The resulting file contains the values of the main factors instead of the values of indicators.

4. The prediction of hydrocarbon potentials consists of three consecutive steps including the generation of a reference sampling calculation of a mathematical model of the reservoir, and estimation of oil and gas reserves.

4.1 The sampling of reference vectors is reduced to generating the STANDARD file which contains all data on oil and gas potentials (total- and net sand thickness and primary oil reserves in a productive formation); the file also contains the values of the main factors calculated with respect to the given drill site.

4.2 The calculation of the mathematical model from the STANDARD file can be carried out either by the well-known technique of pattern recognition or by mathematical modelling of an oil reservoir. The result is stored in the MODEL file which includes regression coefficients and diffusion matrices as well.

Mathematical modelling is based on the assumption that the hydrocarbon potentials of an oil/gas reservoir can be expressed in terms of a current reserve estimate $g(X, Y, G)$, which is a function of the X and Y co-ordinates of observation points, and a set of geological, geophysical and geochemical information available at the sites. The matrix representation has the form

$$\Phi a^{(v)} \lesseqgtr S^{(v)}, \quad v = 1,2 \tag{1}$$

where Φ is the matrix of indicators, which are functions of the X, Y co-ordinates of the observation points and observed geological, geophysical and geochemical fields; each row of matrix Φ is one observation point; $a^{(v)}$ are the column vectors of regression coefficients of local models forming a complete model of a reservoir; $S^{(1)}$ is the difference between the reservoir top and the true or supposed oil–water or gas–water contact and $S^{(2)}$ is the thickness of the oil-bearing layer.

4.3 The estimation of oil and gas potentials includes calculation of the nominal values and probability of an oil/gas deposit, prediction errors at a given level of significance, and extreme (guaranteed and probable) estimates of oil and gas potentials at the same level of significance.

The calculation is made solving the system of the equalities and inequalities (1) with respect to the column vector of the reservoir.

5. A complete set of the calculated local reserve estimates consists of three response surfaces inserted into one another and resting on the common zero-datum plane. The regions of their validity (projected on the horizontal plane) form the proven, probable and possible areas of oil reserves.

The integrated parameters — volumetric parameters and reserves estimates — are calculated analogously with the area estimates, resulting in the proven, probable and possible volumes and reserves of the reservoir.

6. The planning of an exploratory drilling program includes the subdivision of the territory and the estimation of the probability of oil and gas occurrence jointly analysed by the experts.

6.1 The subdivision of the territory is made in the space of the main factors by the methods of set-analysis.

6.2 The probability of oil (and gas) occurrence is calculated taking into account the values obtained from the first and second local models ($v = 1,2$; see 4.3). The results are plotted as maps. The maximum probability points are selected as sites for drilling.

7. The planning of a prospecting drilling program consists of three steps.

7.1 In the first step, certain vectors of the file of the main factors belonging to wells, containing oil and gas at the interval concerned, are selected from the STANDARD file with all due allowances for the MODEL file.

7.2 In the second step, a set of the PREDICTED main factors characterizing the points lying within an inferred oil outline is generated from the file of the main factors with all due allowances for the MODEL file.

7.3 In the third step the mean- and covariance vectors, formed from the main factors in steps 7.1 and 7.2 are compared, and all points are classified in order of preference.

Commonly, the purpose at each subsequent step is to drill a well at a site which will minimize the error of oil reserve estimation. In real situations, however, other purposes can be set, such as maximization of oil reserve addition, minimization of the error of reservoir approximation, and others.

Minimization of the error of reservoir approximation is accomplished by trial and error and by simple comparison of the estimates of the local uncertainty of the reservoir's model.

It is assumed that a well drilled at the site of the maximum preferability will tap a deposit of the calculated total or net thickness, or calculated reserves. Then the mathematical model of the deposit is calculated again producing another drill site and so on.

The solution of problems 2 and 6 is required only for EACS and problem 7 — only for PACS. The other problems (1, 3, 4, 5) are related to both.

The block construction of the system allows one to choose between several combinations of the procedures at each step, in particular to use deterministic processes along with statistical ones.

3. Case histories

The system was tested in the Botuobinski oil and gas bearing province (south-western Yakutiya) and in Belorussia. In the latter case, *(Fig. 3.)* the system was applied to oil prospecting within the Rechitski tract in the northern part of the Pripyat depression, where the known oil occurrences are confined to large-amplitude highs bounded by faults, and occur in intermittent limestones and dolomites lying between salt beds.
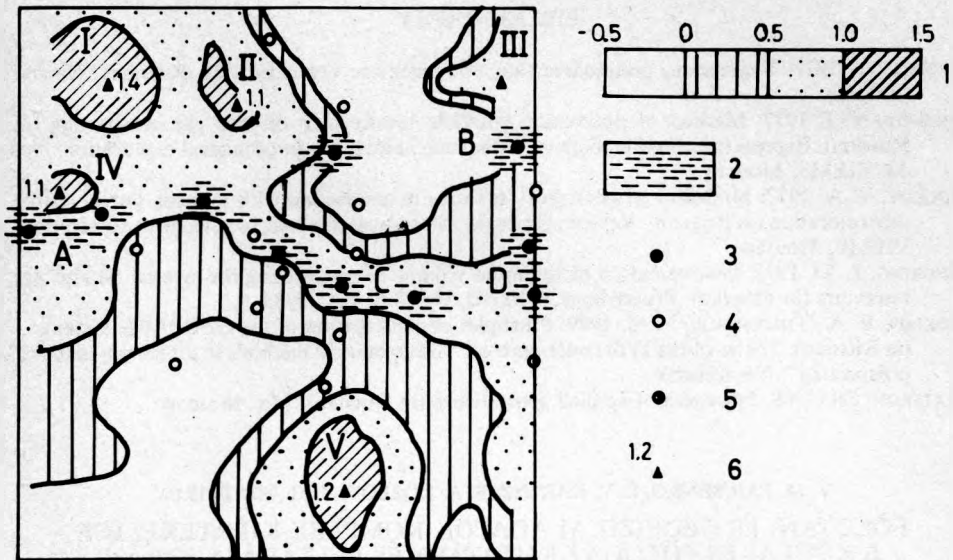
Fig. 3. Scheme for selecting sites for exploratory wells:
1 — scale of hydrocarbon content coefficient (the ratio of nominal estimate of effective oil-saturated thickness to its error); 2 — known oil fields. Deep wells: 3 — productive, 4 — dry, 5 — previously recommended, 6 — recommended by COMPACK, hydrocarbon content indicated

3. ábra. A feltáró fúrások helyét kijelölő eljárás menete
1 — a szénhidrogén-tartalom együttható skálája (az effektív olajjal telített vastagság névleges becslésének a hibához viszonyított értéke); 2 — ismert olajmezők. Mélyfúrások: 3 — produktív, 4 — meddő, 5 — korábban javasolt, 6 — a COMPACK által javasolt (szénhidrogén-tartalom jelölve)

Рис. 3. Схема планирования сети поискового бурения.
1 — шкала значений коэффициента нефтегазоносности — отношения номинальной оценки эффективной нефтенасыщенной мощности к ее ошибка; 2 — известные месторождения нефти. Глубокие скважины: 3 — продуктивные, 4 — непродуктивные, 5 — запроектированные ранее, 6 — рекомендованные, с указанием коэффициента нефтегазоносности

The COMPACK application helped:
— to distinguish complex anomalies of the "oil reservoir" type;
— to select a pattern of exploratory wells within the located anomalies.

The initial matrix of indicators included the depths to the Turonian and Cenomanian reflector, the ΔT values of the geomagnetic field, the Δg Bouguer anomaly values, the temperatures at 50 m, and the values of an integrated geochemical index. Well logs were available, and inflow tests had been made in 23 exploratory and prospecting wells available in the region.

Processing of these data with the COMPACK resulted in the location of five "oil reservoir" type anomalies where the probability of tapping a reservoir containing hydrocarbons exceeded 70%. Six sites for exploratory wells and one for a prospecting well were recommended at the maximum preferability points of these areas.

Two wells were drilled after recommendations and both proved the prediction.

BIBLIOGRAPHY

ALBERT, A. 1977: Regression, pseudoinversion and recursive evaluation (in Russian). Nauka, Moscow

ARONOV, V. I. 1977: Method of optimizing borehole locations in oil and gas prospecting (in Russian). Express information, Series: Mathematical methods in geological exploration, No. 12. VIÉMS, Moscow

VOLKOV, V. A. 1977: Modelling of geological horizons in connection with locating boreholes for oil exploration (in Russian). Review, Series: Mathematical methods in geological exploration. VIÉMS, Moscow

KNORING, L. D. 1977: Determination of optimum volume of prospecting for layered oil and gas reservoirs (in Russian). Proceedings VNIGRI, No. 395. pp. 16–23

KOZLOV, E. A., TIKHOMIROV, V. M. 1979: Principles of construction of the GEOPACK system... (in Russian). Theses of the IVth conference on "Mathematical methods in direct raw material prospecting", Novosibirsk

MATERON, ZH. 1968: Principles of applied geostatistics (in Russian). Mir, Moscow

V. Ju. ZAJCSENKO, E. V. KARUSZ, E. A. KOZLOV, V. M. TIHOMIROV

FÖLDTANI ÉS GEOFIZIKAI ADATOK KOMPLEX KIÉRTÉKELÉSE A KŐOLAJ ÉS FÖLDGÁZ KUTATÁSA ÉS FELTÁRÁSA SORÁN

A földtani, geofizikai és geokémiai adatok komplex kiértékelésének feladatát — a kőolaj- és földgázkutató fúrások előkészítését megelőzően — speciális eljárások sorozatával oldják meg. A folyamat fő lépései: az olaj szempontjából reménybeli terület körvonalazása; a szénhidrogén-potenciál mennyiségi becslése; a rezervoár paramétereinek (méret, alak, szénhidrogén-tartalom) becslése és a feltáró fúrások helyének kijelölése.

A leírt eljárás végrehajtása az erre a célra kifejlesztett programcsomagon alapul, melyet két szénhidrogén-telepen próbáltak ki a gyakorlatban.

В. Ю. ЗАЙЧЕНКО, Е. В. КАРУС, Е. А. КОЗЛОВ, В. М. ТИХОМИРОВ

КОМПЛЕКСНАЯ ИНТЕРПРЕТАЦИЯ ГЕОЛОГО-ГЕОФИЗИЧЕСКИХ ДАННЫХ ПРИ ПОИСКАХ И РАЗВЕДКЕ НЕФТЕГАЗОПЕРСПЕКТИВНЫХ ОБЪЕКТОВ

Задача комплексной интерпретации геолого-геофизических и геохимических данных при подготовке к поисковому разведочному бурению нефтегазоперспективных объектов сведена к последовательности преобразований, включающих формирование пространства признаков наличия залежи, количественный прогноз нефтегазоносности, оценку параметров объектов (размер, форма, степень нефтегазонасыщения), планирование размещения поисковых и разведочных скважин. Технология обработки основана на применении специализированного пакета программ. Дан пример применения технологии.